JAERI-Research
97-073

EFFECTS OF PRIMARY RECOIL (PKA) ENERGY SPECTRUM ON RADIATION DAMAGE IN FCC METALS

October 1997

Tadao IWATA* and Akihiro IWASE

日本原子力研究所
Japan Atomic Energy Research Institute

本レポートは，日本原子力研究所が不定期に公刊している研究報告書です。
入手の問合わせは，日本原子力研究所研究情報部研究情報課（〒319-11 茨城県那珂郡東海村）あて，お申し越しください。なお，このほかに財団法人原子力弘済会資料センター（〒319-11 茨城県那珂郡東海村日本原子力研究所内）で複写による実費頒布をおこなっております。

This report is issued irregularly.
Inquiries about availability of the reports should be addressed to Research Information Division, Department of Intellectual Resources, Japan Atomic Energy Research Institute, Tokai-mura, Naka-gun, Ibaraki-ken 319-11, Japan.

編集兼発行　日本原子力研究所
印　　刷　㈱原子力資料サービス

Effects of Primary Recoil (PKA) Energy Spectrum on Radiation Damage in fcc Metals

Tadao IWATA* and Akihiro IWASE

Advanced Science Research Center
(Tokai Site)
Japan Atomic Energy Research Institute
Tokai-mura, Naka-gun, Ibaraki-ken

(Received September 19, 1997)

Irradiation effects by different energetic particles such as electrons, various ions and neutrons are compared in fcc metals, particularly in Cu and Ni. It is discussed on the statistical consideration that the logarithm of the so-called PKA median energy, log $T_{1/2}$, is a good representative to characterize the primary recoil (i. e. PKA) energy spectrum with the resultant defect production. For the irradiations of electrons, various ions and neutrons to Cu and Ni, fundamental physical quantities such as the fraction of stage I recovery, the defect production cross sections and the radiation annealing cross sections can be well scaled as a function of log $T_{1/2}$, if the effects of the electron excitation caused by irradiating ions are excluded. Namely, all data of the respective physical quantity lie on a single continuous curve as a function of log $T_{1/2}$. This characteristic curve is utilized to predict the damage accumulation (i. e. defect concentration) as a function of dpa in Cu and Ni with the PKA median energy as a parameter.

Keywords: Damage Correlation, Primary Recoil Spectrum, Defect Production, Radiation Annealing, fcc Metals, Stage I Recovery, Damage Accumulation

---

*Research Consultant

金属の照射損傷における反跳原子（PKA）エネルギースペクトル効果

日本原子力研究所先端基礎研究センター
岩田　忠夫*・岩瀬　彰宏

（1997年9月19日受理）

本研究は、核融合14MeV中性子による材料の照射損傷を既存の放射線源を利用した照射実験から予測するために、いわゆる照射損傷の相互比較の物理的枠組を構築することを目的としている。われわれは、照射イオンの種類とエネルギーを大幅に変えて各種の極低温イオン照射実験を行い、欧米で行われた極低温電子照射実験および極低温原子炉中性子照射実験の結果も合わせて、この相互比較の物理的枠組の構築に成功した。照射粒子が異なると、反跳原子（PKA）のエネルギースペクトルが異なるが、その結果生成される照射損傷を特徴づけるパラメータとしてPKAメディアンエネルギーという量を定義した。従来行われてきた照射損傷のDPA評価から出発する場合、照射粒子の相違によるDPA評価からのずれがこのPKA メディアンエネルギーを尺度として統一的に記述できる。

日本原子力研究所（東海駐在）：〒319-11　茨城県那珂郡東海村白方白根2－4
＊　研究嘱託

Contents

目　　次

1 INTRODUCTION

We are concerned with the quantitative correlation of the defect production and radiation annealing in fcc metals irradiated with disparate energetic particles such as electrons, neutrons and various ions. It is of practical importance that we can predict radiation effects in fusion neutron and other new irradiation environments based on the reasonable correlation scheme and the presently available irradiation data from the existing irradiation facilities of electrons, fission neutrons and various ions.[1]

The first step in producing radiation effects is the generation of a primary recoil (i. e. PKA=Primary Knock-on Atom) by the collision of an irradiating energetic particle with a lattice atom or by a nuclear reaction.[2,3] Different irradiation environments result in different PKA energy spectra. However, the atomic displacements initiated by one PKA with a given energy are the same, irrespective of irradiating particles.

The quantity of "dpa" (displacements per atom) has been used as a common scale for the correlation of different irradiations. For any combination of an irradiating particle and a target solid, dpa is defined as $\sigma_d(\mathrm{cal})\,\phi$, where ϕ is the fluence of irradiating particles. $\sigma_d(\mathrm{cal})$ is the calculated displacement (i. e. defect production) cross section. At present, it is calculated on the basis of the modified Kinchin-Pease model, known as the NRT model,[4] which is generally accepted as the international standard for quantifying the number of atomic displacements in irradiated materials. Thus, dpa can be considered to be a kind of fluence weighted with $\sigma_d(\mathrm{cal})$, although it has no dimension.

In the NRT model it is assumed that (i) the atomic displacements are caused by elastic collisions and the effects of electron excitations can be neglected, and (ii) the atomic displacements are randomly dispersed. In reality, however, when the PKA energy becomes high and the number of displacements produced by one PKA increases, the spatial distribution of displacements becomes localized

so that the recombination of unstable Frenkel pairs increases. This localized displacements are not taken into account in the NRT model and therefore in the present dpa calculation. Hence, the ratio of the number of experimentally determined displacements to that of calculated ones, often called the damage efficiency, decreases with increasing PKA energy. This is one of the PKA energy spectrum effects which is expressed as a deviation from the dpa calculation. If we can define a single parameter which characterizes the PKA energy spectrum and its resultant displacements, the radiation effects in different environments can be well correlated by using both dpa and this parameter. We will show that the logarithm of the so-called PKA median energy[5] is a good candidate for it.

To extract the effects of PKA energy spectrum on atomic displacements, in this paper we discuss the stage I recovery, the defect production cross sections and the radiation annealing cross sections in fcc metals, where the PKA energy spectrum is systematically varied by using the different irradiations of electrons, neutrons and various ions. In the stage I recovery of fcc metals,[6] only single interstitial atoms migrate and recombine with vacancies, and the other interstitial clusters are hardly changed. Therefore, the fraction of stage I recovery gives a measure for the fraction of single interstitial atoms in all the displacement cascades which survived the radiation annealing. As mentioned above, the experimental cross section for defect production deviates from σ_d(cal) with increasing PKA energy. Some of defects produced by irradiations are annihilated by subsequent irradiations; this phenomenon is called "radiation annealing". The radiation annealing cross section has not been calculated reliably at present. The experimental values of these cross sections are often discussed by normalizing them with σ_d(cal). If the fraction of stage I recovery, the normalized defect production cross sections and the normalized radiation annealing cross sections are dominated by the effects of PKA energy spectrum, they can be well scaled by the PKA median energy.

Energetic irradiating ions cause the violent electron excitation along their

paths. Through the electron excitation these ion irradiations can contribute to the defect production and radiation annealing even in fcc metals,[7-14] particularly in thin samples which are often used in the case of ion irradiations. This contribution is not taken into the dpa calculation on the NRT model and the present calculations of the PKA energy spectrum. In ion irradiations it is necessary to separate the defect production and radiation annealing due to the electron excitation by irradiating ions from those due to elastic atomic collisions; data on the latter atomic collisions should be used for the correlation of radiation effects between different kinds of irradiations. The degree of electron excitation by irradiating ions is given by the electronic stopping power. If the fraction of stage I recovery, the defect production cross sections and the radiation annealing cross sections are dominated by the electron excitation, they can be well scaled by the electronic stopping power.

On the basis of the present experimental results we try to estimate the damage accumulation (i. e. defect concentration) as a function of dpa for typical irradiations with different PKA median energies. This is important in relation to the accelerated embrittlement observed in ferritic steels at the HFIR pressure vessel location. The present result shows that if the damage accumulation is expressed as a function of dpa, the damage accumulation by irradiations of low energy PKAs such as (n, γ) recoils and γ-induced displacements appears to be accelerated by a factor of about 3 compared with that by irradiations of fission neutrons, where the dependence of the radiation annealing as well as defect production on PKA energy plays an important role.

2 EXPERIMENTAL

The stage I recoveries and the defect production rates were obtained by measuring the electrical resistivity changes. From the defect production rate as a function of fluence, we deduced the defect production cross sections and the

paths. Through the electron excitation these ion irradiations can contribute to the defect production and radiation annealing even in fcc metals,[7-14] particularly in thin samples which are often used in the case of ion irradiations. This contribution is not taken into the dpa calculation on the NRT model and the present calculations of the PKA energy spectrum. In ion irradiations it is necessary to separate the defect production and radiation annealing due to the electron excitation by irradiating ions from those due to elastic atomic collisions; data on the latter atomic collisions should be used for the correlation of radiation effects between different kinds of irradiations. The degree of electron excitation by irradiating ions is given by the electronic stopping power. If the fraction of stage I recovery, the defect production cross sections and the radiation annealing cross sections are dominated by the electron excitation, they can be well scaled by the electronic stopping power.

On the basis of the present experimental results we try to estimate the damage accumulation (i. e. defect concentration) as a function of dpa for typical irradiations with different PKA median energies. This is important in relation to the accelerated embrittlement observed in ferritic steels at the HFIR pressure vessel location. The present result shows that if the damage accumulation is expressed as a function of dpa, the damage accumulation by irradiations of low energy PKAs such as (n, γ) recoils and γ-induced displacements appears to be accelerated by a factor of about 3 compared with that by irradiations of fission neutrons, where the dependence of the radiation annealing as well as defect production on PKA energy plays an important role.

2 EXPERIMENTAL

The stage I recoveries and the defect production rates were obtained by measuring the electrical resistivity changes. From the defect production rate as a function of fluence, we deduced the defect production cross sections and the

radiation annealing cross sections.

It is assumed that the electrical resistivity increase, $\Delta\rho$, is proportional to the defect concentration, c; that is, $\Delta\rho=\rho_F c$, where ρ_F is the electrical resistivity of a Frenkel pair. The available evidence indicates that this assumption is nearly valid. First, the defect production rates have been measured during low-temperature irradiations with electrons, neutrons and various ions, and the results have been consistently analyzed on this assumption.[15] In this connection it is shown in section 5 that the initial transient often observed in the production rate curves has a definite physical meaning.[15] Secondly, the kinetic analyses of stage I and III recoveries after the various irradiations on the above assumption give consistent results.[6] Thirdly, the ratios of resistivity increase to other physical properties such as lattice parameter increase, $\Delta a/a$,[16-18] and stored energy release, ΔQ,[19-22] have been measured during the low-temperature irradiations with electrons, deuterons and neutrons and subsequent thermal annealings. The ratio $\Delta\rho/(\Delta a/a)$ was identical during these various irradiations and annealings, and the ratio $\Delta\rho/\Delta Q$ was also identical during annealings after different irradiations. Furthermore, during the stage II recovery in electron-irradiated Cu and Al, analysis of the diffuse x-ray scattering indicates that the interstitials agglomerate to form clusters,[23,24] while the resistivity was nearly constant. All of the above experiments indicate that the resistivity per defect is insensitive to the degree of clustering, at least for relatively small clusters and even for clusters that occur in neutron-generated cascades. Thus, we can assume that the electrical resistivity increase is nearly proportional to the total number of interstitials and vacancies present, irrespective of their detailed arrangement. We use the electrical resistivity change as such in the study of damage correlation.

Irradiations with ～1 MeV ions and ～100 MeV ions have been performed using the JAERI 2 MV Van de Graaff accelerator and the JAERI tandem accelerator at Tokai, respectively. The irradiation apparatus consists of the beam

scanner for both x and y directions, the slit of 3 mm×6 mm, the Faraday cup used for beam alignment and as beam on-off switch, the secondary-electron repeller and the cryostat. The distance between the scanner and the slit is more than 5 m to provide parallel and uniform beams. The cryostat is insulated from the other parts and acts as a Faraday cup for the electrical measurement of beam current. The secondary electrons ejected from the target can not escape from the large cavity of the cryostat, so that the secondary-electron repeller is not needed in practice. This cryostat was originally designed as a calorimeter for the stopping power measurement.[25] The electrically measured beam current was calibrated using the calorimetric method below 10 K, and the results of the two methods agreed very well within the error of 1 %. The sample areal size is 0.6 mm in width and 10 mm in length and the distance between the two voltage terminals is 3.5 mm. The thickness of the samples is much smaller than the projected ranges of the ions. There are no intervening window foils before the sample. This irradiation system allows us to get the high accuracy for the defect production rate measurement. The preparation of thin samples, the energy loss of ions in samples and the size effect correction for electrical resistivity have been described in the previous papers.[7-14]

Most of the present data have already been presented in the previous papers, where we have primarily been concerned with the effects of electron excitation caused by irradiating ions on the defect production and radiation annealing. In this paper, the data are reexamined and compared with the electron and the neutron irradiation data obtained by other groups with an emphasis on the PKA energy spectrum effects.

3 DPA, AND PKA MEDIAN ENERGY

3. 1 DPA

scanner for both x and y directions, the slit of 3 mm×6 mm, the Faraday cup used for beam alignment and as beam on-off switch, the secondary-electron repeller and the cryostat. The distance between the scanner and the slit is more than 5 m to provide parallel and uniform beams. The cryostat is insulated from the other parts and acts as a Faraday cup for the electrical measurement of beam current. The secondary electrons ejected from the target can not escape from the large cavity of the cryostat, so that the secondary-electron repeller is not needed in practice. This cryostat was originally designed as a calorimeter for the stopping power measurement.[25] The electrically measured beam current was calibrated using the calorimetric method below 10 K, and the results of the two methods agreed very well within the error of 1 %. The sample areal size is 0.6 mm in width and 10 mm in length and the distance between the two voltage terminals is 3.5 mm. The thickness of the samples is much smaller than the projected ranges of the ions. There are no intervening window foils before the sample. This irradiation system allows us to get the high accuracy for the defect production rate measurement. The preparation of thin samples, the energy loss of ions in samples and the size effect correction for electrical resistivity have been described in the previous papers.[7-14]

Most of the present data have already been presented in the previous papers, where we have primarily been concerned with the effects of electron excitation caused by irradiating ions on the defect production and radiation annealing. In this paper, the data are reexamined and compared with the electron and the neutron irradiation data obtained by other groups with an emphasis on the PKA energy spectrum effects.

3 DPA, AND PKA MEDIAN ENERGY

3. 1 DPA

As stated above, dpa can be taken to be a common fluence, weighted with σ_d(cal), for the damage correlation; that is,

$$\text{dpa} = \sigma_d(\text{cal})\ \phi, \tag{1}$$

where ϕ is the fluence. Hence, estimate of dpa is reduced to the calculation of σ_d(cal). For the sake of later discussion, first we describe briefly the calculation of σ_d(cal):

$$\sigma_d(\text{cal}) = \int_{T_d}^{T_m} \nu(T)\ \frac{d\sigma(E,\ T)}{dT}\ dT\ , \tag{2}$$

where $d\sigma(E,T)/dT$ is the differential scattering cross section for an irradiating particle with energy E to produce a PKA with energy T through elastic collisions. The function $\nu(T)$, often called the damage function, is the average total number of Frenkel pairs produced in the atom-atom collisions initiated by a PKA of energy T. Then, T_m is the maximum energy of PKAs, and T_d is the average threshold energy for atomic displacements.

In the case of ion irradiations, Lindhard et al. derived the following approximate form of the differential scattering cross section for screened Coulomb interaction between an irradiating ion and a target atom:[26]

$$\frac{d\sigma(E,\ T)}{dT} = \frac{\pi a^2 \eta E}{2}\ \frac{f(t^{1/2})}{t^{3/2}}\ , \tag{3}$$

where

$$a = 0.8853\ a_0 / (Z_1^{2/3} + Z_2^{2/3})^{1/2} \qquad (a_0 :\ \text{Bohr radius})$$

$$t = \varepsilon^2 T / T_m$$

$$\varepsilon = \left(\frac{M_2 E}{M_1 + M_2}\right)\left(\frac{Z_1 Z_2 e^2}{a}\right)^{-1}$$

$$T_m = 4M_1M_2E / (M_1 + M_2)^2$$

$$\eta = \varepsilon^2 / T_m E = (M_2/M_1)\,(2Z_1Z_2e^2/a)^{-2}\ ,$$

Z_1 and Z_2 are the atomic numbers of the irradiating ion and target atom, M_1 and M_2 are the atomic masses, respectively, and e is the charge of the electrons. The function $f(t^{1/2})$ has been calculated for the Thomas-Fermi potential and tabulated in ref. 26. Its analytical approximation is given by[27]

$$f(t^{1/2}) = \lambda t^{1/6}\left[1 + (2\lambda t^{2/3})^{2/3}\right]^{-3/2} \qquad (\lambda = 1.309)$$

For $t \gg 1$, this differential scattering cross section is reduced to the Rutherford scattering cross section.

In the case of electron irradiations, for $\alpha = Z_2/137 \ll 1$, the differential scattering cross section is[2,3]

$$\frac{d\sigma(E, T)}{dT} = \frac{\pi b^2}{4}\frac{T_m}{T^2}\left\{1 - \beta^2\frac{T}{T_m} + \pi\alpha\beta\left[\left(\frac{T}{T_m}\right)^{1/2} - \frac{T}{T_m}\right]\right\}, \qquad (4)$$

where

$$b = 2Z_2e^2(1 - \beta^2)^{1/2} / m_eV^2, \qquad \beta = V/c,$$
$$T_m = 2(m_e / M_2)(E + 2m_ec^2) E / m_ec^2,$$

m_e is the mass of the electron, V is the velocity of irradiating electrons, and c is the velocity of light. The above equations for electron irradiations include relativistic effects.

In the case of neutron irradiations, the differential cross sections are not given as compact analytical formulas. We have to utilize the nuclear data files such as ENDF/B and the computer codes.[28-30]

In the NRT model,[4] the inelastic energy loss is calculated according to the theory of Lindhard et al.[31] and its analytical approximation.[32] Then, the function $\nu(T)$ is given by a modified Kinchin-Pease expression:

$$\nu(T) = \begin{cases} 0, & T < T_d \\ 1, & T_d \le T < 2.5\ T_d \\ \dfrac{0.8\ T}{1 + \kappa\ g(\varepsilon)}\ \dfrac{1}{2\ T_d}, & T \ge 2.5\ T_d \end{cases} \qquad (5)$$

where

$$g(\varepsilon) = 3.4008\ \varepsilon^{1/6} + 0.40244\ \varepsilon^{3/4} + \varepsilon\ ,$$
$$\kappa = 0.1337\ Z_2^{2/3} / A_2^{1/2}\ ,$$
$$\varepsilon = T / \left(86.93\ Z_2^{7/3}\right), \qquad (T \text{ in eV})$$

and A_2 is the mass number of the target atom. In eq. (5) it is assumed that only the kinetic energy deposited in elastic atomic collisions results in damage and the electron excitations are dissipated only as heat.

3. 2 PKA Median Energy

We discuss what is a good representative of the PKA energy spectrum based on the statistical consideration. The PKA energy spectrum as a function of T for a unit fluence is the differential scattering cross section, $d\sigma(E,T)/dT$.

The average value of the PKA energy with this spectrum is given by

$$T_{av}(E) = \frac{\displaystyle\int_{T_d}^{T_m} T\ \frac{d\sigma(E,\ T)}{dT}\ dT}{\displaystyle\int_{T_d}^{T_m} \frac{d\sigma(E,\ T)}{dT}\ dT}\ . \qquad (6)$$

For ion and electron irradiations, the differential scattering cross sections given by eqs. (3) and (4) are abnormal distributions which diverge steeply with decreasing T. It is invalid to take the average of these abnormal distributions. Therefore, the average PKA energy, $T_{av}(E)$, is not a good representative of the

PKA energy spectrum.

Next, we consider the PKA energy spectrum weighted with the damage function $\nu(T)$ for a unit fluence, as a function of T: [10]

$$F(T)\,dT = \nu(T)\,\frac{d\sigma(E,\,T)}{dT}\,dT\,, \tag{7}$$

where for brevity the variable E is omitted in F(T). The function F(T) represents the distribution of atomic displacements due to the PKA energy spectrum, and we need to know its representative. However, F(T) still diverges with decreasing T. Therefore, it is not appropriate to take a representative of this abnormal distribution.

Then, by putting $X = \log T$ and $dX = dT/T$, we transform F(T) into the following distribution as a function of X;

$$G(X)\,dX = \nu(e^X)\,\frac{d\sigma(E,\,e^X)}{dX}\,dX\,, \tag{8}$$

where

$$\int_{T_d}^{T_m} F(T)\,dT \;=\; \int_{X_d}^{X_m} G(X)\,dX \;=\; \sigma_d(\mathrm{cal})\,, \tag{9}$$

$X_d = \log T_d$ and $X_m = \log T_m$. The function G(X) does not diverge and is not abnormal. Hence, we can take the median as a representative of this distribution function. The median $X_{1/2}$ is defined by

$$\int_{X_{1/2}}^{X_m} G(X)\,dX \;=\; \frac{1}{2}\int_{X_d}^{X_m} G(X)\,dX\,. \tag{10}$$

Here, $X_{1/2} = \log T_{1/2}$, and $T_{1/2}$ is usually called the PKA median energy. Then, eq. (10) is equivalent to the familiar definition of $T_{1/2}$; [5]

$$\int_{T_{1/2}}^{T_m} \nu(T) \frac{d\sigma(E, T)}{dT} dT = \frac{1}{2} \int_{T_d}^{T_m} \nu(T) \frac{d\sigma(E, T)}{dT} dT = \frac{1}{2} \sigma_d(\mathrm{cal}) . \quad (11)$$

In other words, half of the displaced atoms result from PKAs with energies higher than $T_{1/2}$.

Hence, in the cases of ion and electron irradiations, we can take the logarithm of the PKA median energy, $\log T_{1/2}$, as a good representative to characterize the PKA energy spectrum weighted with the resultant displacements.

Figures 1 to 3 show the distribution functions G(X) and their median $X_{1/2}$ for the typical cases of electron, ion and neutron irradiations in Cu. We adopt 29 and 33 eV as T_d for Cu and Ni, respectively.[33] The discontinuity in curves at $X=\log(2.5\ T_d)$ comes from the discontinuity in the definition of $\nu(T)$ at $T=2.5\ T_d$ in eq. (5). At present, there is no consensus as to how to treat this point.

In section 6 we show that, for irradiations of electrons, various ions and neutrons, the fraction of stage I recovery, the normalized defect production cross sections and the normalized radiation annealing cross sections can be well scaled by $\log T_{1/2}$, if they are not affected by the electron excitation due to irradiating ions.

4 STAGE I RECOVERY AND TYPES OF FRENKEL PAIRS

When typical fcc metals such as Cu and Ni are irradiated at low temperatures below 10 K (where interstitial atoms and vacancies are immobile) and then heated to successively higher temperatures, several recovery stages are observed. They are commonly designated as stages I, II, III, IV and V. Stage I

$$\int_{T_{1/2}}^{T_m} \nu(T) \frac{d\sigma(E, T)}{dT} dT = \frac{1}{2} \int_{T_d}^{T_m} \nu(T) \frac{d\sigma(E, T)}{dT} dT = \frac{1}{2} \sigma_d(\mathrm{cal}) . \quad (11)$$

In other words, half of the displaced atoms result from PKAs with energies higher than $T_{1/2}$.

Hence, in the cases of ion and electron irradiations, we can take the logarithm of the PKA median energy, $\log T_{1/2}$, as a good representative to characterize the PKA energy spectrum weighted with the resultant displacements.

Figures 1 to 3 show the distribution functions G(X) and their median $X_{1/2}$ for the typical cases of electron, ion and neutron irradiations in Cu. We adopt 29 and 33 eV as T_d for Cu and Ni, respectively.[33] The discontinuity in curves at $X=\log(2.5\ T_d)$ comes from the discontinuity in the definition of $\nu(T)$ at $T=2.5\ T_d$ in eq. (5). At present, there is no consensus as to how to treat this point.

In section 6 we show that, for irradiations of electrons, various ions and neutrons, the fraction of stage I recovery, the normalized defect production cross sections and the normalized radiation annealing cross sections can be well scaled by $\log T_{1/2}$, if they are not affected by the electron excitation due to irradiating ions.

4 STAGE I RECOVERY AND TYPES OF FRENKEL PAIRS

When typical fcc metals such as Cu and Ni are irradiated at low temperatures below 10 K (where interstitial atoms and vacancies are immobile) and then heated to successively higher temperatures, several recovery stages are observed. They are commonly designated as stages I, II, III, IV and V. Stage I

recovery, typically below 80 K, is most prominent and has been intensively studied.[6]

To our present knowledge, the stage I recovery in fcc metals shows most clearly the differences in radiation effect caused by irradiations of different particles such as electrons, various ions and neutrons.

Figure 4 compares the stage I recovery in Cu after irradiations of (a) 2 MeV electrons,[34] (b) various ions[12] and (c) fission neutrons,[35] in which the resistivity changes by irradiations, $\Delta\rho_0$, are about 0.134 nΩ cm, 300 nΩ cm and 2 nΩ cm, respectively. If we assume ρ_F=2.0x10^{-4} Ω cm for Cu,[36] the respective defect concentrations are 0.67 ppm, 1500 ppm and 10 ppm. The ordinate is the temperature derivative of the resistivity recovery curve $\Delta\rho/\Delta\rho_0$. The abscissa is the annealing temperature.

In the case of electron irradiations, stage I recovery consists of five substages, I_A~I_E. On the other hand, in the case of fission neutron irradiations, substages I_A, I_B and I_C are largely reduced compared with the case of electron irradiations. Then, in the cases of ion irradiations, substages are reduced from the low-temperature side as the mass (or to a lesser extent, the energy) of irradiating ions is increased. The cases of various ion irradiations are between two extreme cases of the electron and the neutron irradiations.

Strictly, the relative intensity of substages depends on the defect concentration, $\Delta\rho_0/\rho_F$, produced by irradiations. However, if we compare many recovery data accumulated till now, we can conclude that the relative intensity of substages depends more on the type of irradiating particles than the defect concentration. Therefore, in spite of the large differences in defect concentration, stage I recoveries in Fig. 4 give a qualitative comparison of radiation effects between different irradiating particles. In other words, they clearly show one of the PKA energy spectrum effects.

In stage I, interstitial atoms become mobile and recombine with immobile

vacancies. As discussed below, substages in stage I can be considered to correspond to the annealing of different types of Frenkel pairs, which differ in the relative configuration of interstitial atoms and vacancies.

An interpretation of the substages in electron-irradiated Cu was proposed by Corbett, Smith and Walker (CSW),[37,38] which has been widely accepted. In the CSW model, I_A, I_B and I_C are due to the recombination of close Frenkel pairs, I_D is associated with the recombination of freely migrating interstitial atoms with their own vacancies (correlated recombination) and I_E associated with the recombination of freely migrating interstitial atoms with other vacancies (uncorrelated recombination). In I_E, some of the freely migrating interstitial atoms can also react with other interstitials or impurities, thereby being trapped in the form of immobile clusters. They attempted to identify the specific configurations of close Frenkel pairs responsible for I_A, I_B and I_C by evaluating the elastic interaction energy between Frenkel pairs. On the other hand, Holder et al. proposed a model for the I_C close-pair configuration based on measurements of changes in the elastic constants and their temperature dependences.[39,40]

The peak for substage I_D is much wider than would be expected for a single activation energy with a constant frequency factor. There was once a controversy concerning the interpretation of the peak-broadening in I_D. CSW analyzed their data using the Waite theory and reached the above interpretation.[41] The theory is based upon the assumption of a unique activation energy and accounts for the width of the peak in terms of the initial radial distribution function describing the separation of interstitial atoms and vacancies. The key point of CSW data is that the initial portion of the I_D isothermals is proportional to the square root of the recovery time, precisely as required by the Waite theory of correlated recovery. On the other hand, Granato and Nilan (GN) interpreted I_D as a superposition of additional,

unresolved close-pair recombinations,[42] that is, a distribution of activation energies with negligible variation in frequency factor.

We show that the GN model also can interpret the peak-broadening in I_D quantitatively.[43] For simplicity, we approximate a distribution of activation energies by a Gaussian distribution,

$$\frac{1}{(2\pi)^{1/2}\,\varepsilon}\exp\left[-\frac{(E-E_0)^2}{2\,\varepsilon^2}\right],$$

where E is the activation energy and ε means the width of the activation energy distribution. Then, if we put with CSW[41] E_0=0.117 eV and the frequency factor of 1.2×10^{12} sec^{-1}, and further assume ε/E_0=0.06, we can well reproduce not only the initial $t^{1/2}$ dependence but also the whole curves of the I_D isothermals measured by CSW, and, therefore, can reproduce the whole peak structure (or the peak temperature, the half width, etc.) of the I_D isochronal peak. Generally, when we consider an annealing process within the framework of a chemical rate equation, the interpretation of the peak-broadening in terms of a distribution of activation energies seems to be much easier and more natural than that in terms of a distribution of frequency factors; the latter coresponds to the Waite theory.

The peaks of I_A, I_B and I_C for ion irradiations are broadened compared with those for electron irradiations when the defect concentrations produced by the respective irradiations are nearly the same. As the PKA energy increases, the atomic displacements increase and another defect is produced near any one Frenkel pair. For ion irradiations, the activation energies for the recombination of close Frenkel pairs may be slightly changed by the lattice strains due to these nearby defects, that is, there may be a distribution of activation energies. Incidentally, one of the authors proposed a chemical rate equation describing

the annealing process with a distribution of activation energies,[44] applicable to the reaction of higher orders as well as a first order; the equation can be easily extended to describe the annealing process with a distribution of frequency factors.

Recently, Baily et al. performed electron irradiations of thin Cu single crystals near displacement threshold and found that the relative intensity of I_A, I_B and I_C peaks depends on the irradiation direction.[45] They tried to identify the configuration of close Frenkel pairs in each substage by comparing with the results from molecular-dynamics calculations. They also found that the peak temperature of I_D is shifted as a function of irradiation direction, which clearly shows that substage I_D is a superposition of the recombination of a series of Frenkel pairs with different activation energies. It may be difficult to explain such a shift of the I_D peak by assuming a unique activation energy and by varying the form of the initial radial distribution function in the Waite theory.

Substage I_E is observed in electron and light-ion irradiations when the defect concentration produced is low. As the defect concentration increases, I_E merges into I_D. Frenkel pairs in I_E do not have specified configurations, but they can be classified as a group of Frenkel pairs which are annihilated by uncorrelated recombination.

On the basis of these experiments and calculations, we can define five types of Frenkel pairs in terms of substages I_A～I_E, although the detailed configuration of the respective pairs still remains to be investigated.

5 DEFECT PRODUCTION RATE AND DETERMINATION OF CROSS SECTIONS

One of the most fundamental physical quantities in radiation effects is the

the annealing process with a distribution of activation energies,[44] applicable to the reaction of higher orders as well as a first order; the equation can be easily extended to describe the annealing process with a distribution of frequency factors.

Recently, Baily et al. performed electron irradiations of thin Cu single crystals near displacement threshold and found that the relative intensity of I_A, I_B and I_C peaks depends on the irradiation direction.[45] They tried to identify the configuration of close Frenkel pairs in each substage by comparing with the results from molecular-dynamics calculations. They also found that the peak temperature of I_D is shifted as a function of irradiation direction, which clearly shows that substage I_D is a superposition of the recombination of a series of Frenkel pairs with different activation energies. It may be difficult to explain such a shift of the I_D peak by assuming a unique activation energy and by varying the form of the initial radial distribution function in the Waite theory.

Substage I_E is observed in electron and light-ion irradiations when the defect concentration produced is low. As the defect concentration increases, I_E merges into I_D. Frenkel pairs in I_E do not have specified configurations, but they can be classified as a group of Frenkel pairs which are annihilated by uncorrelated recombination.

On the basis of these experiments and calculations, we can define five types of Frenkel pairs in terms of substages I_A～I_E, although the detailed configuration of the respective pairs still remains to be investigated.

5 DEFECT PRODUCTION RATE AND DETERMINATION OF CROSS SECTIONS

One of the most fundamental physical quantities in radiation effects is the

cross section for defect production, radiation annealing, etc. which has the inverse dimension of the fluence.

These cross sections are defined through the measurement of defect production rate:[46,47]

$$\frac{dc_j}{d\phi} = \sigma_{d,j}\left[1 - v_0 c\right]^2 + \sum_{l \neq j} \sigma_{t,lj}\, c_l - \sum_{l \neq j} \sigma_{t,jl}\, c_j - \sigma_{r,j}\, c_j \ , \qquad (12)$$

where ϕ is the fluence and the indexes j and l denote the type of defects. For the defects of type j, c_j is the defect concentration, $\sigma_{d,j}$ is the defect production cross section (or the displacement cross section), $\sigma_{t,jl}$ is the defect transformation cross section from type j into type l, and $\sigma_{r,j}$ is the radiation annealing cross section. Then, v_0 is the spontaneous recombination volume and c is the total defect concentration, $c = \Sigma_j c_j$.

Figures 5 and 6 show typical examples of the defect production rate (or the damage rate) curves in Cu and Ni, respectively, measured as a function of ion fluence. The ordinate is the resistivity change rate $d(\Delta\rho)/d\phi$, where $\Delta\rho=\rho_F c$. The defect production rate curves can be expressed as the sum of a few exponential functions of the fluence.

Equation (12) is too sophisticated to apply to the analysis of actual experimental results such as given in Figs. 5 and 6. Therefore, we have proposed a simplified equation of defect production rate,[9,10] where the terms containing $\sigma_{t,lj}$ and $\sigma_{t,jl}$ are neglected compared with $\sigma_{r,j}c_j$.

It is assumed that there are several different types of defects produced by irradiations and some of them are annihilated by subsequent irradiations. If the defects of type 1 to type k-1 are unstable against the subsequent irradiations and if the other types of defects, which are stable against them, are put together and designated as defects of type k, the defect production and radiation annealing can be described by the following simultaneous differential

equations:

$$\frac{dc_j}{d\phi} = \sigma_{d,j}\left(1 - 2v_0 c\right) - \sigma_{r,j}\, c_j \qquad \text{for } 1 \le j \le k-1 ,$$

$$\frac{dc_k}{d\phi} = \sigma_{d,k}\left(1 - 2v_0 c\right), \qquad \text{and} \qquad c = \sum_{j=1}^{k} c_j . \tag{13}$$

For pure samples, when $\sigma_{r,j} \gg 2v_0\sigma_{d,j}$, the approximate solution of eq. (13) is

$$c_j \cong \frac{\sigma_{d,j}}{\sigma_{r,j}} \left\{ \exp[-2v_0\sigma_{d,k}\phi] - \exp[-(\sigma_{r,j} + 2v_0\sigma_{d,j})\phi] \right\} \quad \text{for } 1 \le j \le k-1 ,$$

$$c_k \cong \frac{1}{2v_0} \left\{ 1 - \exp[-2v_0\sigma_{d,k}\phi] \right\} , \tag{14}$$

and

$$\frac{dc}{d\phi} \cong \sum_{j=1}^{k-1} \sigma_{d,j} \exp[-(\sigma_{r,j} + 2v_0\sigma_{d,j})\phi] + \sigma_{d,k} \exp[-2v_0\sigma_{d,k}\phi] . \tag{15}$$

By fitting eq. (15) to the defect production rate curves, we can determine the defect production cross sections, $\sigma_{d,j}$, and the radiation annealing cross sections, $\sigma_{r,j}$. These cross sections will be examined in section 6. 2 as a function of the logarithm of PKA median energy, or as a function of the electronic stopping power for irradiating ions

In section 4, we defined the types of Frenkel pairs in terms of substages of stage I recovery. On the basis of the present formulation, the type of defects can also be defined in terms of the component of defect production rate curves. As shown in Figs. 5 and 6, two or three types of defects can be identified in Cu and Ni by the defect production rate measurement. At present, there are few experiments concerning the correspondence of the defect types determined in both definitions. Then, c_j in eq. (14) should be associated with the peak intensity of stage I substages.

For doped samples, the approximate solution of eq. (13) is given in refs. 9 and 10. We measured both stage I～III recovery and defect production rate in pure

and doped samples of Cu and Ni using 100 MeV Iodine ion irradiations.[8] In this case, a satisfactory correspondence was obtained between the types of defects determined in both measurements, and the radiation annealing cross sections of the respective types of defects by the Iodine irradiations were determined. Duesing et al.[46,47] performed a detailed study on the defect production in Al, Cu and Pt irradiated with 2.8 and 3 MeV electrons by measuring the defect production rates and stage I recovery, where they utilized skillfully the radiation doping, subthreshold irradiation and partial thermal annealing. They determined the radiation annealing cross sections of the respective types of close Frenkel pairs by electron irradiations, the spontaneous recombination volume, etc.

6 EFFECTS OF PKA ENERGY SPECTRUM

6. 1 Fraction of Stage I Recovery

In most cases, it is difficult to quantitatively saparate stage I recovery into substages. Therefore, we consider the total of stage I recovery summed over substages. Then, the fraction of stage I recovery in the whole recovery stages gives a measure for the fraction of single interstitial atoms in all the displacement cascades.

Figures 7 and 8 compare the fraction of stage I recovery in Cu and Ni, respectively, as a function of the logarithm of PKA median energy, $\log T_{1/2}$, after irradiations with electrons, various ions or fission neutrons. The defect concentrations produced by the respective irradiations are nearly the same; they are about 300 and 500 nΩ cm in resistivity unit, that is, about 1500 and 830 ppm in Cu and Ni, respectively, where we assume $\rho_F=6\times10^{-4}$ Ω cm for Ni.[36]

In the case of Cu shown in Fig. 7, all data of the fraction of stage I recovery lie on the one curve which decreases gradually with increasing $\log T_{1/2}$. Data

and doped samples of Cu and Ni using 100 MeV Iodine ion irradiations.[8] In this case, a satisfactory correspondence was obtained between the types of defects determined in both measurements, and the radiation annealing cross sections of the respective types of defects by the Iodine irradiations were determined. Duesing et al.[46,47] performed a detailed study on the defect production in Al, Cu and Pt irradiated with 2.8 and 3 MeV electrons by measuring the defect production rates and stage I recovery, where they utilized skillfully the radiation doping, subthreshold irradiation and partial thermal annealing. They determined the radiation annealing cross sections of the respective types of close Frenkel pairs by electron irradiations, the spontaneous recombination volume, etc.

6 EFFECTS OF PKA ENERGY SPECTRUM

6. 1 Fraction of Stage I Recovery

In most cases, it is difficult to quantitatively saparate stage I recovery into substages. Therefore, we consider the total of stage I recovery summed over substages. Then, the fraction of stage I recovery in the whole recovery stages gives a measure for the fraction of single interstitial atoms in all the displacement cascades.

Figures 7 and 8 compare the fraction of stage I recovery in Cu and Ni, respectively, as a function of the logarithm of PKA median energy, $\log T_{1/2}$, after irradiations with electrons, various ions or fission neutrons. The defect concentrations produced by the respective irradiations are nearly the same; they are about 300 and 500 nΩ cm in resistivity unit, that is, about 1500 and 830 ppm in Cu and Ni, respectively, where we assume $\rho_F=6\times10^{-4}$ Ω cm for Ni.[36]

In the case of Cu shown in Fig. 7, all data of the fraction of stage I recovery lie on the one curve which decreases gradually with increasing $\log T_{1/2}$. Data

for irradiations with electrons, various ions, and fission neutrons are from ref. 48, refs. 7 and 12-14, and ref. 50, respectively. The figure shows that (1) the logarithm of PKA median energy is a good scaling parameter to compare the fraction of stage I recovery among the widely different irradiations, and (2) as the PKA energy increases, the fraction of single interstitial atoms produced in the displacement cascades decreases and the fraction of clustered interstitial atoms increases. We conclude that the shape of curve in Fig. 7 is characteristic of the PKA energy spectrum effect.

The stage I recovery data for fusion neutron irradiations to nearly the same defect concentration as in Fig. 7 have not been obtained. Roberto et al.[51] measured the stage I recovery in Cu after the irradiation of d-Be neutrons with a broad peak near 15 MeV to the defect concentration of about 1 nΩ cm, and compared its result with their relevant fission neutron result, where the respective PKA median energies are about 300 keV and 70 keV. The fraction of stage I recovery was nearly the same for these two irradiations, which suggests that the curve of Fig. 7 becomes flat between these two energies. The constancy of the stage I recovery fraction is consistent with the concept of subcascade formation that increasing the PKA energy above a few 10 keV only increases the number of subcascades.

Next, in the case of Ni shown in Fig. 8, data of the fraction of stage I recovery for irradiations with electrons, various ions, and fission neutrons are from ref. 52, refs. 7 and 12-14, and refs. 53 and 54, respectively. All the data, except for ～ 100 MeV heavy-ion irradiations, lie on a single curve similar to the one for Cu. Namely, they can be well scaled by log $T_{1/2}$ and this dependence of the stage I recovery fraction on log $T_{1/2}$ represents the PKA energy spectrum effect.

On the other hand, the data for ～100 MeV heavy-ion irradiations, together with the data for ～1 MeV ion irradiations, can be well scaled by the electronic stopping power for irradiating ions.[7] Namely, the radiation annealing due to the electron excitation by these irradiating ions results in the anomalous reduction

of the stage I recovery fraction in Ni irradiated with ～100 MeV heavy ions, where the effect of electron excitation is overwhelmingly larger than that of atomic collisions.

In Al, Ag and Pt also, the fraction of stage I recovery has been studied as a function of log $T_{1/2}$.[12,13]

6. 2 Defect Production Cross Sections and Radiation Annealing Cross Sections

When we compare the experimental data of defect production rates for irradiations of electrons, various ions and neutrons, there are some problems to be solved such as the correspondence of defect types observed in the respective irradiations, the separation of type k defects from others (or determination of v_0), etc. In order to compare these diverse data at the present stage, we simplify eq. (15) as follows;

$$\frac{dc}{d\phi} \cong \sum_{j=1} \sigma_{d,j} \exp\left(- \sigma_{r,j} \phi \right), \qquad (16)$$

where the terms $2v_0\sigma_{d,j}$ are included in $\sigma_{r,j}$. Equation (16) is necessary and adequate to the analysis of defect production rate data.

6. 2. 1 Cross sections in Cu Figure 9 shows the defect production cross sections $\sigma_{d,j}$ and the radiation annealing cross sections $\sigma_{r,j}$, normalized with σ_d(cal), as a function of log $T_{1/2}$ for irradiations with electrons,[46] various ions[11,14,55] and neutrons in Cu. Data of the cross sections for neutron irradiations have been evaluated from refs. 50 and 56-59.

We notice that these cross sections are measured by using the resistivity

change, which is, as mentioned in section 2, assumed to be proportional to the total defect concentration, irrespective of whether the defects are isolated or clustered. On the other hand, the fraction of stage I recovery gives the fraction of single interstitial atoms in all the displaced atoms.

As shown in Fig. 5, for ion irradiations to Cu two types of defects are identified as two components of defect production rate curves. We designate them as defects of types 1 and 2 in order of appearance as the fluence increases. Then, data for electron and neutron irradiations are considered to correspond to defects of type 2 for ion irradiations. The initial transient of defect production rate curves has often been observed in electron and neutron irradiations,[15] but it has been usually neglected in the analysis of previous works.

As for defects of type 2, the normalized defect production cross sections, $\sigma_{d,2}/\sigma_d$(cal), for irradiations of electrons, various ions and neutrons, lie on one smooth curve which decreases monotonically from near 1 at low energies to about 0.3 for energies above a few 10 keV. This behavior can be explained in the framework of elastic collisions as follows. If the NRT model is valid, the normalized cross sections (i. e. the damage efficiency) should be 1; even if considering the uncertainty in the values of T_d and ρ_F used for the calculation of σ_d(cal) and defect concentration, they should be constant. In reality, however, as the PKA energy increases, the number of displacements in the displacement cascades produced by one PKA increases and the spatial density of displacements becomes high, so that some of displaced atoms are annihilated by recombining with other vacancies spontaneously, and the efficiency of defect production decreases compared with the NRT model. The constancy above a few 10 keV is a consequence of subcascade formation. Thus, we can consider that this trend of the normalized cross sections represents typically one of the PKA energy spectrum effects.

The normalized cross sections for radiation annealing of defects of type 2, $\sigma_{r,2}/\sigma_d$(cal), show the same trend as a function of log $T_{1/2}$ as those for defect production, except that the former are more than two orders of magnitude larger

than the latter. We can conclude that the defect production and radiation annealing of defects of type 2 in Cu are governed by elastic atomic collisions.

As for defects of type 1 in Cu, the normalized cross sections both for defect production and for radiation annealing, $\sigma_{d,1}/\sigma_d$(cal) and $\sigma_{r,1}/\sigma_d$(cal), show a peculiar behavior as a function of log $T_{1/2}$ for ～1 MeV ion irradiations as well as for ～100 MeV ion irradiations. Rather, as Figs. 10(a) and (b) show clearly, the defect production cross sections and radiation annealing cross sections, $\sigma_{d,1}$ and $\sigma_{r,1}$, are functions of the electronic stopping power S_e for irradiating ions, and they are proportional to $S_e^{1.7}$ and $S_e^{1.3}$, respectively. We can conclude that the defect production and radiation annealing for defects of type 1 in Cu are governed by the electron excitation.

Although the defect production rate measurements show that the defects of type 1 are due to the electron excitation, we can not find any peculiar shift in the stage I recovery curve as a function of log $T_{1/2}$ in Fig. 7. The reason may be as follows. The defect concentration produced by irradiations is given by the integral of eq. (16) as a function of fluence. In the case of ion irradiations of the stage I recovery measurements in Cu, the concentration of type 1 defects produced was about 0.1 or less of that of type 2 defects. Hence, it is considered that, because the fractional concentration of type 1 defects was small, we could not observe the effect of electron excitation on stage I recovery in Cu with the present accuracy of measurements.

In Ag also, the defect production rate curves consist of two components; namely, the production and radiation annealing of two types of defects are observed.[11,14] The dependence of the respective cross sections on log $T_{1/2}$ or Se in Ag is similar to that in Cu.

6. 2. 2 Cross sections in Ni　　Figure 11 shows the normalized defect production cross sections and the normalized radiation annealing cross sections

for irradiations with various ions[55] and fission neutrons in Ni. Data of the cross sections for fission neutron irradiations have been evaluated from refs. 50 and 56-58.

For ～1 MeV ion irradiations, two types of defects are identified as two components of defect production rate curves; they are designated as defects of types 1* and 2 in order from the low fluence side. On the other hand, for ～100 MeV ion irradiations three types of defects are identified as three components of the curves. There is, however, some ambiguity in the separation of the initial two components, so we put them together and designate them as defects of type 1*, where $\sigma_{d,\,1}{}^{*}$ is the sum of $\sigma_{d,\,j}$ for the two components and $\sigma_{r,\,1}{}^{*}$ is the average of $\sigma_{r,\,j}$ between them weighted with the respective $\sigma_{d,\,j}$. Then, defects corresponding to the third component is designated as defects of type 2.

In Fig. 11 are shown the normalized defect production cross sections, summed over defects of types 1* and 2, that is, $(\sigma_{d,\,1}{}^{*}+\sigma_{d,\,2})/\sigma_{d}(\mathrm{cal})$. Data for ～1 MeV ion irradiations lie on the solid curve which is nearly proportional to the curve for $\sigma_{d,\,2}/\sigma_{d}(\mathrm{cal})$ of Cu in Fig. 9, although the absolute values differ between the two curves because of the uncertainty of T_d and ρ_F adopted. The normalized defect production cross sections for fission neutron irradiations are also situated on this curve. Hence, we can conclude that the solid curve shows the typical dependence of the normalized defect production cross sections on $\log T_{1/2}$, where the defect production is due to atomic collisions.

On the other hand, the normalized defect production cross sections for ～100 MeV ion irradiations are reduced as shown by the broken curve compared with the corresponding cross sections for ～1 MeV ion irradiations. This means that there are some types of defects which are once produced by atomic collisions but annihilated by subsequent irradiations and therefore can not be observed experimentally. The conditions to detect the production and radiation annealing of the specified defects in pure and doped samples have been discussed in ref. 9. If for defects of type j the cross section for radiation

annealing is overwhelmingly larger than that for defect production, that is, $\sigma_{d,j}/\sigma_{r,j} \ll 1$, the productin of such defects can not be observed experimentally.

The normalized radiation annealing cross sections of defects of type 2, $\sigma_{r,2}/\sigma_d(\mathrm{cal})$, also show two different dependences on log $T_{1/2}$ as shown by the solid and the broken curve. We consider that the normalized cross sections for ～1 MeV ion irradiations and fission neutron irradiations shown by the solid curve are characteristic of the PKA energy spectrum effect. Data for ～100 MeV ion irradiations shown by the broken curve are reduced compared with the solid curve. The reduction of radiation annealing for ～100 MeV ion irradiations may be due to the defect transformation from other types into type 2 during irradiation, which can not be treated by the simplified formulation of eq. (13).

As for the normalized radiation annealing cross sections of defects of type 1*, $\sigma_{r,1}^*/\sigma_d(\mathrm{cal})$, all data for both ～1 MeV and ～100 MeV ion irradiations lie on a single curve which is considered to be characteristic of the PKA energy spectrum effect.

In any case, we conclude that the defect production and radiation annealing observed by the present defect production rate measurements in pure Ni are governed by atomic elastic collisions.

As mentioned before, we measured the defect production rates for irradiation of 100 MeV I-ions in pre-doped samples of Ni and Cu.[8] In pre-doped Ni, we observed the radiation annealing of three types of defects and the respective normalized cross sections for radiation annealing were 3.9×10^4, 8.4×10^3 and 1.3×10^3. The normalized cross section of 1.3×10^3 agrees well with the relevant cross section of 1.4×10^3 observed in pure Ni and plotted in Fig. 11. The values of 3.9×10^4 and 8.4×10^3 observed in pre-doped Ni could not be detected in pure Ni. We consider that these larger cross sections for radiation annealing in Ni are due to the electron excitation and they result in the

anomalous reduction of stage I recovery as mentioned in section 6. 1. In Ni also, it is considered that the electron excitation by energetic irradiating ions can cause the production of some types of defects. However, such defect production may not be observed because of the extraordinarily large cross sections for radiation annealing.

On the other hand, for ～100 MeV I-ion irradiations in pre-doped Cu, we observed the radiation annealing of two types of defects and the respective normalized cross sections for radiation annealing were 2.4×10^{3} and 2.8×10^{2}. These values agree well with the relevant cross sections of 2.5×10^{3} and 1.6×10^{2}, respectively, observed in pure Cu and plotted in Fig. 9.

Incidentally, Noggle et al. measured the defect production rates for Ni ion irradiations to Ni and Fe-17% Cr and found an anomalous reduction of the rates with the defect accumulation for their open beam condition.[60,61] This result was contrasted with their measurement for Al ion irradiations to Al where the rates were not anomalous.[62] We infer based on the present investigation that the anomalous reduction in their case reflects the large radiation annealing due to the electron excitation by irradiating Ni ions.

7 DAMAGE ACCUMULATION AS A FUNCTION OF DPA

In 1986, Charpy V-notch surveillance testing of ferritic steels from the High Flux Isotope Reactor at Oak Ridge National Laboratory revealed significantly more embrittlement than predicted from reference test reactor data.[63] Since then, it has been argued that low energy PKAs produced by (n, γ) reactions[64] or produced via Compton scattering and pair formation by gamma rays[65,66] are more effective for the accelerated embrittlement than high energy PKAs produced by fast neutrons.

As an explanation for the accelerated embrittlement, Mansur and Farrell have

anomalous reduction of stage I recovery as mentioned in section 6. 1. In Ni also, it is considered that the electron excitation by energetic irradiating ions can cause the production of some types of defects. However, such defect production may not be observed because of the extraordinarily large cross sections for radiation annealing.

On the other hand, for ～100 MeV I-ion irradiations in pre-doped Cu, we observed the radiation annealing of two types of defects and the respective normalized cross sections for radiation annealing were 2.4×10^3 and 2.8×10^2. These values agree well with the relevant cross sections of 2.5×10^3 and 1.6×10^2, respectively, observed in pure Cu and plotted in Fig. 9.

Incidentally, Noggle et al. measured the defect production rates for Ni ion irradiations to Ni and Fe-17% Cr and found an anomalous reduction of the rates with the defect accumulation for their open beam condition.[60,61] This result was contrasted with their measurement for Al ion irradiations to Al where the rates were not anomalous.[62] We infer based on the present investigation that the anomalous reduction in their case reflects the large radiation annealing due to the electron excitation by irradiating Ni ions.

7 DAMAGE ACCUMULATION AS A FUNCTION OF DPA

In 1986, Charpy V-notch surveillance testing of ferritic steels from the High Flux Isotope Reactor at Oak Ridge National Laboratory revealed significantly more embrittlement than predicted from reference test reactor data.[63] Since then, it has been argued that low energy PKAs produced by (n, γ) reactions[64] or produced via Compton scattering and pair formation by gamma rays[65,66] are more effective for the accelerated embrittlement than high energy PKAs produced by fast neutrons.

As an explanation for the accelerated embrittlement, Mansur and Farrell have

considered the spectral effect that point defects produced in small cascades from (n, γ) and (n, α) reactions generally avoid in-cascade recombination, while most of the defects created in large cascades produced by fast neutrons are lost to in-cascade recombination.[64] They have discussed the relative availability of migrating point defects, which avoid in-cascade recombination, as a function of PKA energy. Rehn et al. have proposed the concept of freely-migrating defects,[65,67] in which only a fraction of the total number of defects that are generated by irradiation actually become free to migrate over substantial distances. Based on solute segregation measurements at elevated temperatures, they have obtained the relative efficiency for producing freely-migrating defects as a function of PKA median energy, where the efficiency decreases strongly with increasing PKA energy.

On the other hand, recent dosimetry experiments revealed the presence of an intense gamma field at the HFIR surveillance locations[68] and, if so, this hitherto uncounted gamma rays may be the main cause of the higher-than-expected embrittlement observed there. However, the problem of PKA energy effects still remains to be clarified quantitatively.

Using the experimental cross sections obtained in the previous section, we calculated the defect concentration (i. e. damage accumulation) in Cu and Ni as a function of dpa with the PKA median energy as a parameter. The defect concentration is given by the integral of eq. (16);

$$c \cong \sum_{j=1} \frac{\sigma_{d,j}}{\sigma_{r,j}} \left\{ 1 - \exp\left(- \frac{\sigma_{r,j}}{\sigma_d(\mathrm{cal})} [\mathrm{dpa}] \right) \right\} , \qquad (17)$$

where $[\mathrm{dpa}] = \sigma_d(\mathrm{cal})\, \phi$.

When we try to predict the changes in properties caused by neutron irradiations or other new irradiations based on ion irradiation experiments, we have to exclude the property changes ascribed to the electron excitation by irradiating ions, so that the defect productions and radiation annealings can be

compared between different irradiations within the framework of elastic collisions. In the present case, we consider the production and radiation annealing of defects of type 2 in Cu and those of defects of types 1* and 2 in Ni. We choose 0.6 keV as a low PKA median energy which is typical of (n, γ) recoils or gamma induced displacements and choose 35 keV as a high PKA median energy which is typical of displacements in usual fission reactors. The cross sections used in the calculation are given in Table I. If we can assume that the embrittlement is proportional to the defect concentration, the results are applicable to the assessment of the effects of PKA energy on the embrittlement.

Figure 12 shows the calculated results. If compared at the defect concentration of around 1×10^{-3}, dpa for the PKA median energy of 0.6 keV is about 1/3 of dpa for that of 35 keV in Cu and Ni. In other words, if the damage accumulation (i. e. defect concentration) is expressed as a function of dpa, the accumulation for low $T_{1/2}$ irradiations appears to be accelerated by a factor of about 3 compared with that for high $T_{1/2}$ irradiations. This acceleration is caused by the dependence of $\sigma_{r,\,2}/\sigma_d$(cal) as well as $\sigma_{d,\,2}/\sigma_{r,\,2}$ on $T_{1/2}$.

In the present calculation, as we used the experimental cross sections measured at low temperatures below 10 K, the results do not contain the effects of thermal annealing and show quantitatively the effects of PKA median energy. Finally, it should be emphasized that the radiation annealing as well as defect production depends on the PKA median energy; this fact has not been explicitly considered in previous discussions of enhanced embrittlement.[63-65,69]

8 SUMMARY

It is shown on the statistical consideration that the logarithm of the so-called PKA median energy, $\log T_{1/2}$, is a good scale for the comparison of the PKA energy spectrum effects among different irradiations.

compared between different irradiations within the framework of elastic collisions. In the present case, we consider the production and radiation annealing of defects of type 2 in Cu and those of defects of types 1* and 2 in Ni. We choose 0.6 keV as a low PKA median energy which is typical of (n, γ) recoils or gamma induced displacements and choose 35 keV as a high PKA median energy which is typical of displacements in usual fission reactors. The cross sections used in the calculation are given in Table I. If we can assume that the embrittlement is proportional to the defect concentration, the results are applicable to the assessment of the effects of PKA energy on the embrittlement.

Figure 12 shows the calculated results. If compared at the defect concentration of around 1×10^{-3}, dpa for the PKA median energy of 0.6 keV is about 1/3 of dpa for that of 35 keV in Cu and Ni. In other words, if the damage accumulation (i. e. defect concentration) is expressed as a function of dpa, the accumulation for low $T_{1/2}$ irradiations appears to be accelerated by a factor of about 3 compared with that for high $T_{1/2}$ irradiations. This acceleration is caused by the dependence of $\sigma_{r,\,2}/\sigma_d$(cal) as well as $\sigma_{d,\,2}/\sigma_{r,\,2}$ on $T_{1/2}$.

In the present calculation, as we used the experimental cross sections measured at low temperatures below 10 K, the results do not contain the effects of thermal annealing and show quantitatively the effects of PKA median energy. Finally, it should be emphasized that the radiation annealing as well as defect production depends on the PKA median energy; this fact has not been explicitly considered in previous discussions of enhanced embrittlement.[63-65,69]

8 SUMMARY

It is shown on the statistical consideration that the logarithm of the so-called PKA median energy, $\log T_{1/2}$, is a good scale for the comparison of the PKA energy spectrum effects among different irradiations.

Experimental data of such fundamental physical quantities as the fraction of stage I recovery, the normalized defect production cross sections and the normalized radiation annealing cross sections are compared in Cu and Ni for irradiations of different energetic particles such as electrons, various ions and neutrons. All the data of the respective physical quantity lie on a single continuous curve as a function of log $T_{1/2}$, if the effects of the electron excitation caused by irradiating ions are excluded. This curve is considered to typically characterize the PKA energy spectrum effect.

This characteristic curve can be used for predicting the defect production and radiation annealing for any irradiation if the PKA energy spectrum is known. As an example which shows the PKA energy spectrum effect, the damage accumulation in Cu and Ni is calculated as a function of dpa with the PKA median energy as a parameter.

ACKNOWLEDGMENTS

This paper is dedicated to Professor S. Ishino with many thanks on the occasion of his retirement from the University of Tokyo. The authors are thankful to Professor T. Nihira of Ibaraki University for many years' cooperation and fruitful discussions, to Dr. T. Aruga of JAERI for calculating the PKA energy spectra for neutron irradiations and to the technical staff of the Accelerators Division, JAERI (Tokai) for operating the JAERI tandem accelerator. One of the authors (T. I.) would also like to express his hearty thanks to the late Dr. K. Tsukada of JAERI and the late Dr. T. S. Noggle of ORNL for encouraging him to start the ion irradiation experiments at low temperatures.

Experimental data of such fundamental physical quantities as the fraction of stage I recovery, the normalized defect production cross sections and the normalized radiation annealing cross sections are compared in Cu and Ni for irradiations of different energetic particles such as electrons, various ions and neutrons. All the data of the respective physical quantity lie on a single continuous curve as a function of log $T_{1/2}$, if the effects of the electron excitation caused by irradiating ions are excluded. This curve is considered to typically characterize the PKA energy spectrum effect.

This characteristic curve can be used for predicting the defect production and radiation annealing for any irradiation if the PKA energy spectrum is known. As an example which shows the PKA energy spectrum effect, the damage accumulation in Cu and Ni is calculated as a function of dpa with the PKA median energy as a parameter.

ACKNOWLEDGMENTS

This paper is dedicated to Professor S. Ishino with many thanks on the occasion of his retirement from the University of Tokyo. The authors are thankful to Professor T. Nihira of Ibaraki University for many years' cooperation and fruitful discussions, to Dr. T. Aruga of JAERI for calculating the PKA energy spectra for neutron irradiations and to the technical staff of the Accelerators Division, JAERI (Tokai) for operating the JAERI tandem accelerator. One of the authors (T. I.) would also like to express his hearty thanks to the late Dr. K. Tsukada of JAERI and the late Dr. T. S. Noggle of ORNL for encouraging him to start the ion irradiation experiments at low temperatures.

REFERENCES

1. F. L. Vook, H. K. Birnbaum, T. H. Blewitt, W. L. Brown, J. W. Corbett, J. H. Crawford, Jr., A. N. Goland, G. L. Kulcinski, M. T. Robinson, D. N. Seidman, F. W. Young, Jr., Report to the American Physical Society by the Study Group on Physics Problems Relating to Energy Technologies: Radiation Effects on Materials, Rev. Mod. Phys., Vol. 47, Suppl. No. 3 (1975).
2. F. Seitz and J. S. Koehler, in Solid State Physics, eds. F. Seitz and D. Turnbull (Academic, New York, 1956), Vol. 2, pp. 305-448.
3. C. Lehmann, Interaction of Radiation with Solids and Elementary Defect Production (North-Holland, Amsterdam, 1977).
4. M. J. Norgett, M. T. Robinson, and I. M. Torrens, Nucl. Eng. Des. **33**, 50 (1975).
5. R. S. Averback, R. Benedek, and K. L. Merkle, Phys. Rev. B **18**, 4156 (1978).
6. W. Schilling, G. Burger, K. Isebeck, and H. Wenzl, in Vacancies and Interstitials in Metals, eds. A. Seeger, D. Schumacher, W. Schilling and J. Diehl (North-Holland, Amsterdam, 1970), pp. 255-361.
7. A. Iwase, S. Sasaki, T. Iwata, and T. Nihira, Phys. Rev. Lett. **58**, 2450 (1987).
8. A. Iwase, T. Iwata, S. Sasaki, and T. Nihira, J. Phys. Soc. Jpn. **59**, 1451 (1990).
9. T. Iwata and A. Iwase, Rad. Effects and Defects Solids **113**, 135 (1990).
10. T. Iwata and A. Iwase, Nucl. Instr. Method **B61**, 436 (1991).
11. A. Iwase, T. Iwata, and T. Nihira, J. Phys. Soc. Jpn. **61**, 3878 (1992).
12. A. Iwase, T. Iwata, T. Nihira, and S. Sasaki, Mater. Sci. Forum **97-99**, 605 (1992).
13. A. Iwase, T. Iwata, T. Nihira, and S. Sasaki, Rad. Effects and Defects Solids **124**, 117 (1992).
14. A. Iwase and T. Iwata, Nucl. Instr. Meth. B **90**, 322 (1994).
15. see references cited in ref. 9.
16. H. Wagner, F. Dworschak, and W. Schilling, Phys. Rev. B **2**, 3856 (1970).
17. E. E. Gruber, J. A. Tesk, T. H. Blewitt, and R. E. Black, Phys. Rev. B **2**, 2849

(1970).

18. F. Dworschak, H. Wagner, and P. Wombacher, Phys. Stat. Sol. (b) **52**, 103 (1972).
19. T. G. Nilan and A. V. Granato, Phys. Rev. **137**, A1233 (1965).
20. R. Losehand, F. Rau, and H. Wenzl, Rad. Effects **2**, 69 (1969).
21. K. Feese, D. Hoffmann, and H. Wollenberger, Cryst. Lattice Defects **1**, 245 (1970).
22. J. M. Cotignola, C. Minier, A. Paillery, and E. Bonjour, Phys. Stat. Sol. **42**, 167 (1970).
23. P. Ehrhart, H.-G. Haubold, and W. Schilling, Advan. Solid State Phys. **14**, 87 (1974).
24. P. Ehrhart and U. Schlagheck, J. Phys. F **4**, 1589 (1974).
25. A. Iwase, S. Sasaki, T. Iwata, and T. Nihira, J. Phys. Soc. Jpn. **54**, 1750 (1985).
26. J. Lindhard, V. Nielsen, and M. Scharff, Kgl. Dan. Vidensk. Selsk. Mat.-fys. Medd. **36**, no. 10 (1968).
27. K. B. Winterbon, P. Sigmund, and J. B. Sanders, Kgl. Dan. Vidensk. Selsk. Mat.-fys. Medd. **37**, no. 14 (1970).
28. D. M. Parkin and A. N. Goland, Rad. Effects **28**, 31 (1976).
29. T. A. Gabriel, J. D. Amburgey, and N. M. Greene, Nucl. Sci. Eng. **61**, 21 (1976).
30. T. Aruga and K. Shiraishi, in Proc. of the 1988 Seminar on Nuclear Data, eds. T. Nakagawa and A. Zukeran (Japan Atomic Energy Research Institute, 1989) JAERI-M 89-026, pp. 342-359.
31. J. Lindhard, V. Nielsen, M. Scharff, and P. V. Thomsen, Kgl. Dan. Vidensk. Selsk. Mat.-fys. Medd. **33**, no. 10 (1963).
32. M. T. Robinson, in Nuclear Fusion Reactors, eds. J. L. Hall and J. H. C. Maple (British Nuclear Energy Society, London, 1970) pp. 364-378.
33. P. Lucasson, in Fundamental Aspects of Radiation Damage in Metals, eds. M. T. Robinson and F. W. Young, Jr., U. S. ERDA CONF-751006-P1 (1976) pp. 42-65.

34. C. L. Snead, Jr., F. W. Wiffen, and J. W. Kauffman, Phys. Rev. **164**, 900 (1967). see also ref. 6.
35. G. Burger, sited in ref. 6.
36. F. W. Young, Jr., J. Nucl. Mater. **69** & **70**, 310 (1978).
37. J. W. Corbett, R. B. Smith, and R. M. Walker, Phys. Rev. **114**, 1452 (1959).
38. J. W. Corbett, R. B. Smith, and R. M. Walker, Phys. Rev. **114**, 1460 (1959).
39. J. Holder, A. V. Granato, and L. E. Rehn, Phys. Rev. Lett. **32**, 1054 (1974).
40. J. Holder, A. V. Granato, and L. E. Rehn, Phys. Rev. B **10**, 363 (1974).
41. J. W. Corbett, Phys. Rev. **137**, A1806 (1965).
42. A. V. Granato and T. G. Nilan, Phys. Rev. **137**, A1250 (1965).
43. T. Iwata, unpublished.
44. T. Iwata, J. Nucl. Mater. **133** & **134**, 361 (1985).
45. A. C. Baily, W. E. King, K. L. Merkle, and M. Meshii, Phys. Rev. B **46**, 8593 (1992).
46. G. Duesing, W. Sassin, W. Schilling, and H. Hemmerich, Cryst. Lattice Defects **1**, 55 (1969).
47. G. Duesing, H. Hemmerich, W. Sassin, and W. Schilling, Cryst. Lattice Defects **1**, 135 (1970).
48. W. Sassin, cited in ref. 49.
49. P. Ehrhart, in Landolt-Börnstein, New Series, Group III: Crystal and Solid State Physics, Vol. 25: Atomic Defects in Metals, ed. H. Ullmaier (Springer-Verlag, Berlin, 1991) Chap. 2. 3.
50. M. Nakagawa, K. Böning, P. Rosner, and G. Vogl, Phys. Rev. B **16**, 5285 (1977).
51. J. B. Roberto, C. E. Klabunde, J. M. Williams, and R. R. Coltman, Jr., J. Nucl. Mater. **73**, 97 (1978).
52. S. K. Khanna and K. Sonnenberg, Rad. Effects **59**, 91 (1981). see also ref. 49.
53. J. A. Horak and T. H. Blewitt, J. Nucl. Mater. **49**, 161 (1973/74); errata, ibid. **50**, 315 (1974).
54. G. Burger, cited in ref. 50.

55. A. Iwase, T. Iwata, and T. Nihira, unpublished.
56. M. A. Kirk and L. R. Greenwood, J. Nucl. Mater. **80**, 159 (1979).
57. R. R. Coltman, Jr., C. E. Klabunde, and J. M. Williams, J. Nucl. Mater. **99**, 284 (1981).
58. C. E. Klabunde and R. R. Coltman, Jr., J. Nucl. Mater. **108 & 109**, 183 (1982).
59. M. W. Guinan and J. H. Kinney, J. Nucl. Mater. **108 & 109**, 95 (1982).
60. T. S. Noggle, B. R. Appleton, J. M. Williams, and T. Iwata, ORNL-5328, Solid State Div. Annu. Prog. Rep. (April 30, 1977) pp. 103-105.
61. T. S. Noggle, D. B. Poker, and B. R. Appleton, ORNL-5640, Solid State Div. Annu. Prog. Rep. (February 29, 1980) pp. 131-132.
62. T. S. Noggle, B. R. Appleton, J. M. Williams, O. S. Oen, T. Iwata, and G. W. Vogl, J. Nucl. Mater. **125**, 330 (1984).
63. R. K. Nanstad, K. Farrell, D. N. Braski, and W. R. Corwin, J. Nucl. Mater. **158**, 1 (1988).
64. L. K. Mansur and K. Farrell, J. Nucl. Mater. **170**, 236 (1990).
65. L. E. Rehn and R. C. Birtcher, J. Nucl. Mater. **205**, 31 (1993).
66. N. P. Baumann, Proc. 7th ASTM-EURATOM Symp. on Reactor Dosimetry, Strasbourg, France, eds. G. Tsotridis, R. Dierckx, and P. D'Hondt (Kluwer Academic, Dordrecht, 1990) pp. 689-697.
67. L. E. Rehn and P. R. Okamoto, Mater. Sci. Forum **15-18**, 985 (1987).
68. I. Remec, J. A. Wang, F. B. K. Kam, and K. Farrell, J. Nucl. Mater. **217**, 258 (1994).
69. K. Farrell, S. T. Mahmood, R. E. Stoller, and L. K. Mansur, J. Nucl. Mater. **210**, 268 (1994).

Table I

Defect production cross sections, $\sigma_{d,j}$, and radiation annealing cross sections, $\sigma_{r,j}$, which are substituted into eq. (17) for calculation of the curves shown in Fig. 12.

PKA median energy (keV)	Cu		Ni			
	$\frac{\sigma_{d,2}}{\sigma_d(cal)}$	$\frac{\sigma_{r,2}}{\sigma_d(cal)}$	$\frac{\sigma_{d,1}^*}{\sigma_d(cal)}$	$\frac{\sigma_{r,1}^*}{\sigma_d(cal)}$	$\frac{\sigma_{d,2}}{\sigma_d(cal)}$	$\frac{\sigma_{r,2}}{\sigma_d(cal)}$
0.6	0.81	300	0.025	6.5×10^3	0.675	200
35	0.30	160	0.02	1.6×10^3	0.27	110

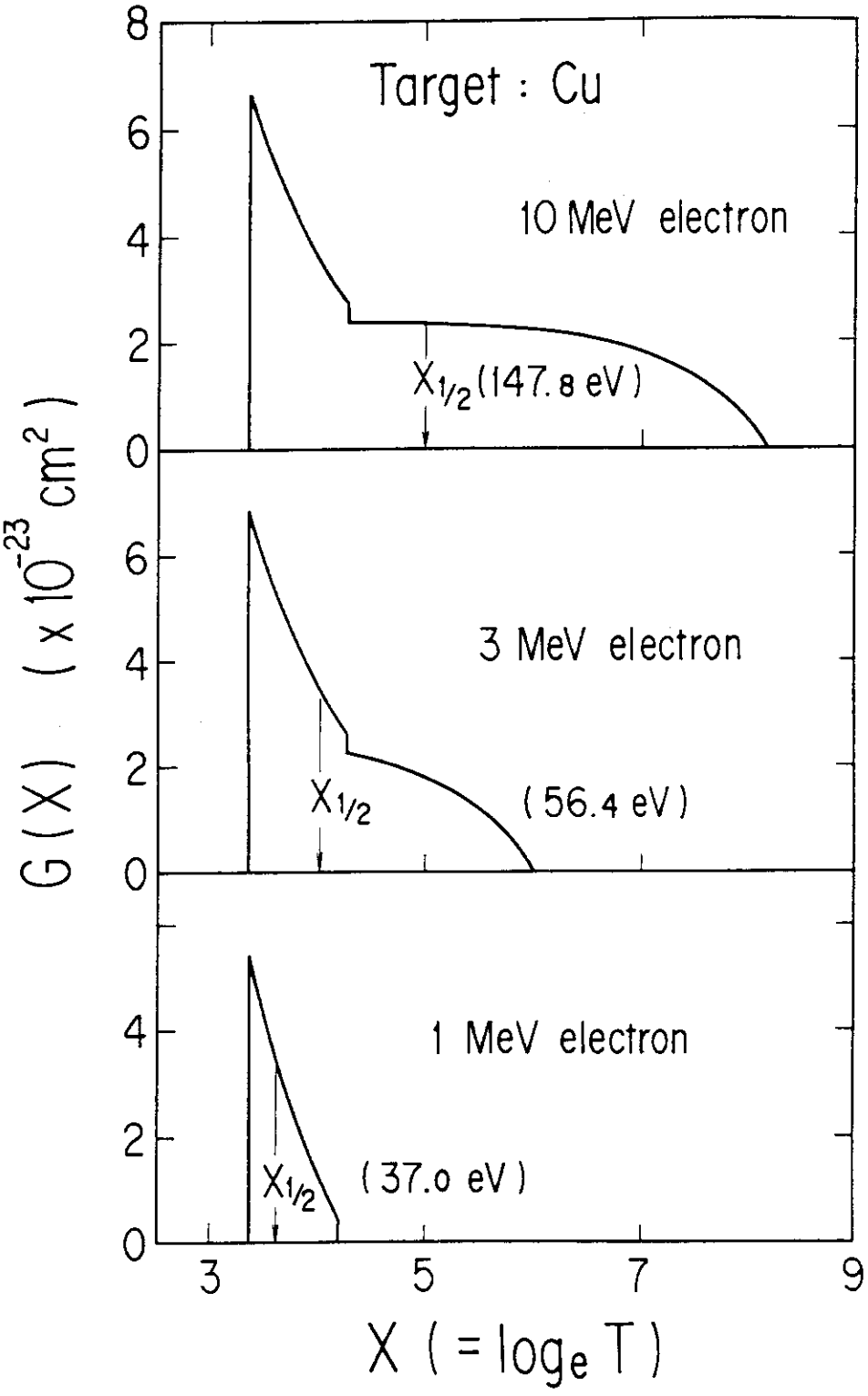

FIGURE 1 Distribution functions G(X) as functions of X(=log T) for electron irradiations to Cu, where T is the PKA energy in eV. Numerical figures in parentheses show the PKA median energies.

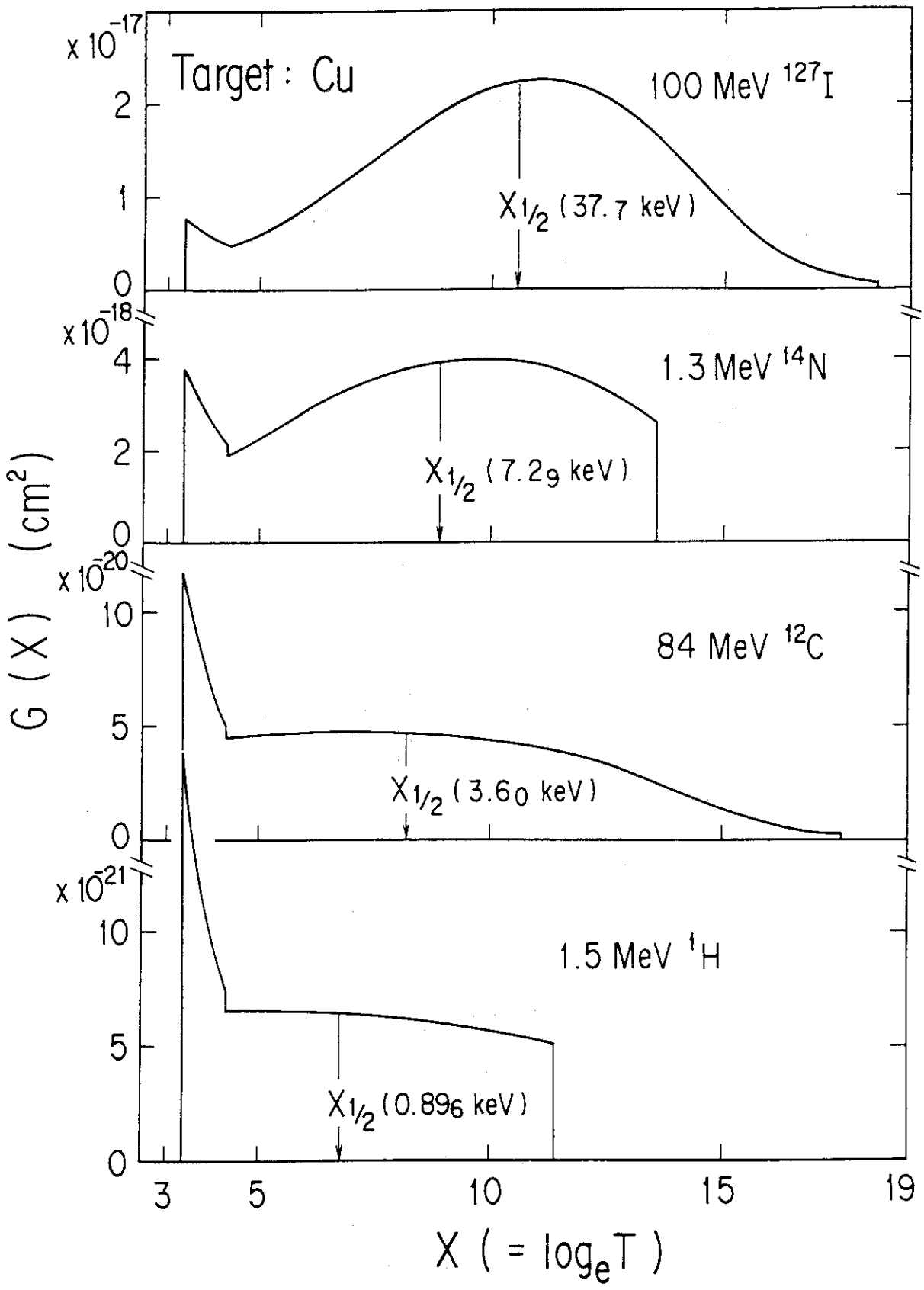

FIGURE 2 Distribution functions G(X) as functions of X(=log T) for various ion irradiations to Cu. Numerical figures in parentheses show the PKA median energies.

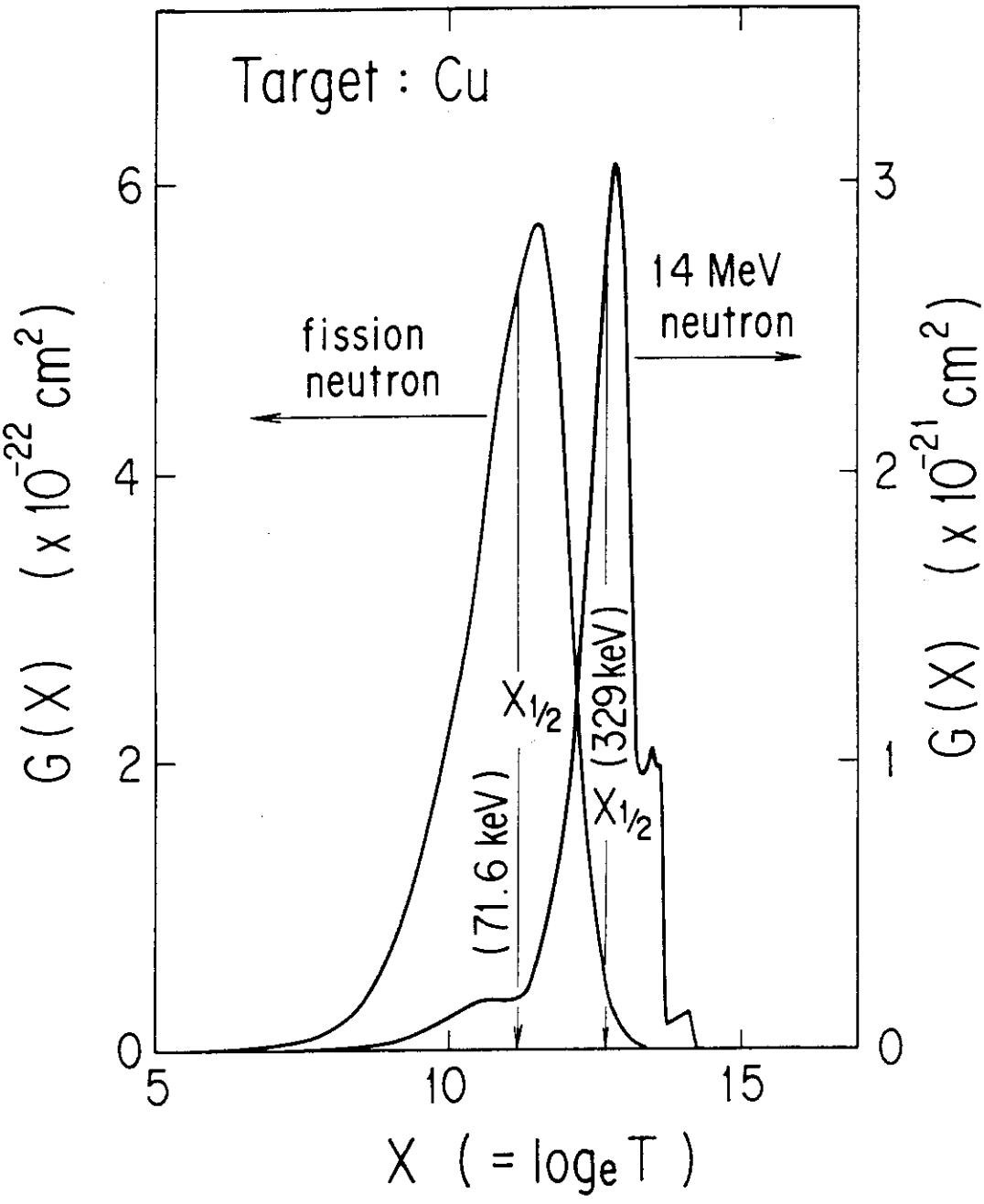

FIGURE 3 Distribution functions G(X) as functions of X(=log T) for fission and fusion neutron irradiations to Cu. Numerical figures in parentheses show the PKA median energies.

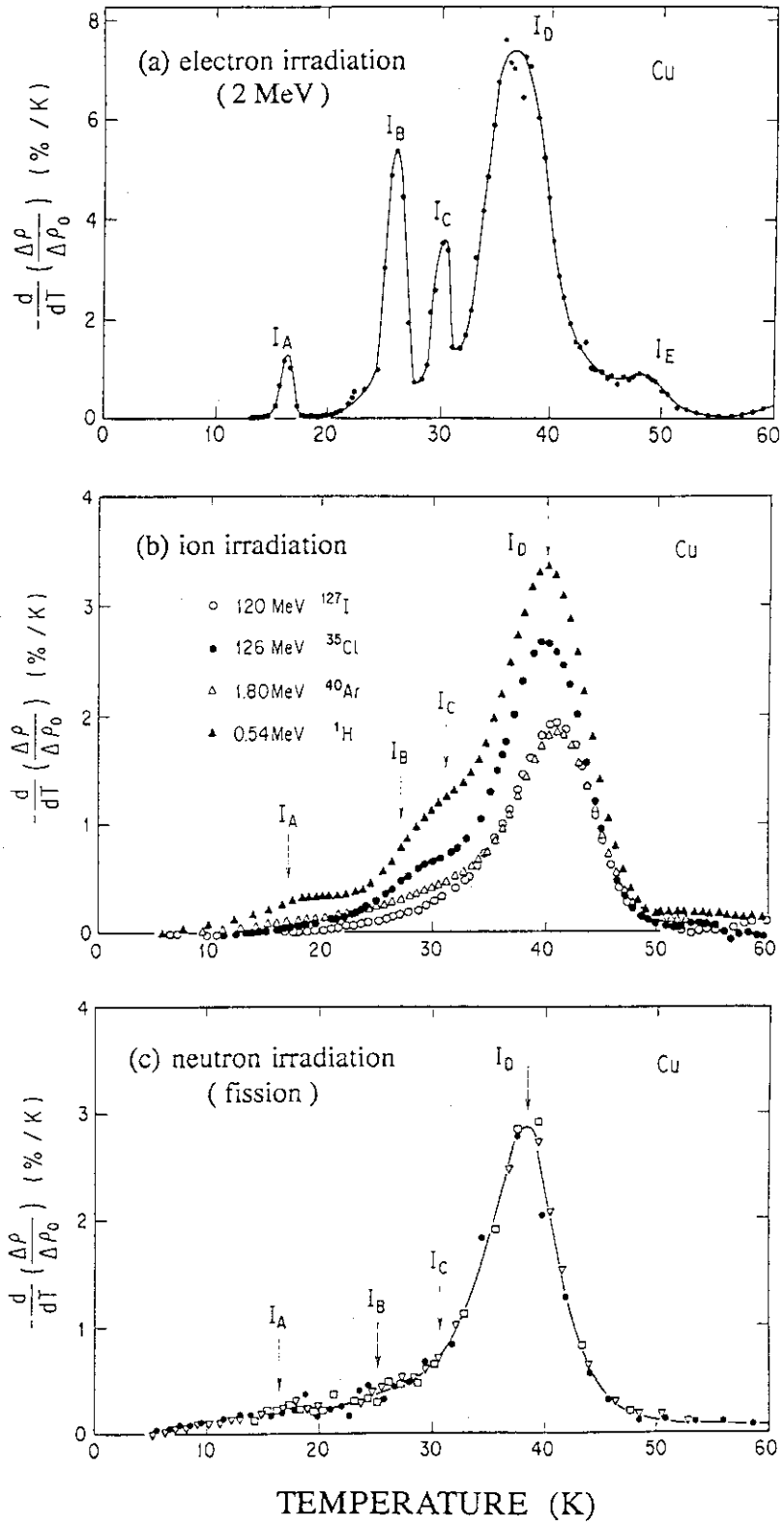

FIGURE 4 Stage I recovery spectra of Cu after low temperature irradiations with (a) 2 MeV electrons, (b) various ions, and (c) fission neutrons. The ordinate is the temperature derivative of the resistivity recovery curve $\Delta\rho/\Delta\rho_0$, where $\Delta\rho_0$ is the resistivity change by irradiations. The abscissa is the annealing temperature.

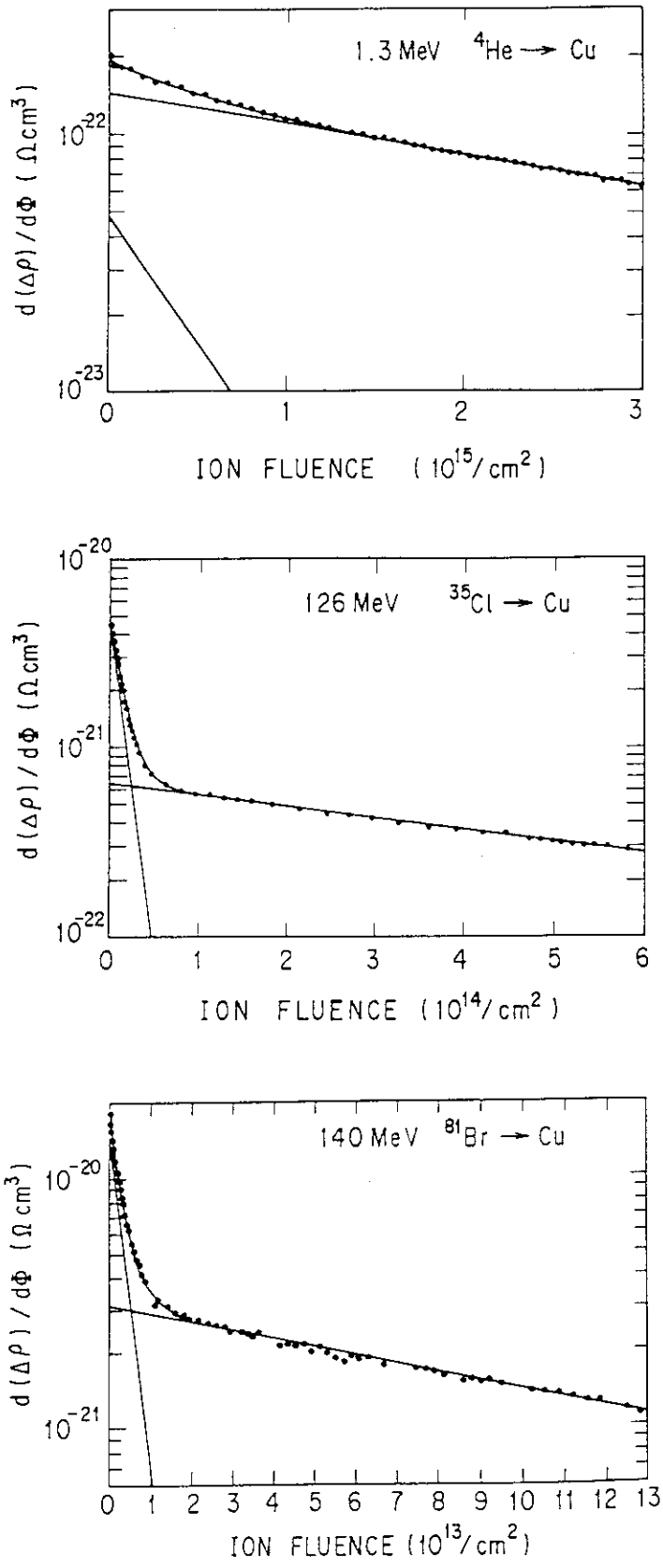

FIGURE 5 Defect production rates as functions of ion fluence for Cu irradiated with 1.3 MeV He ions, 126 MeV Cl ions and 140 MeV Br ions.

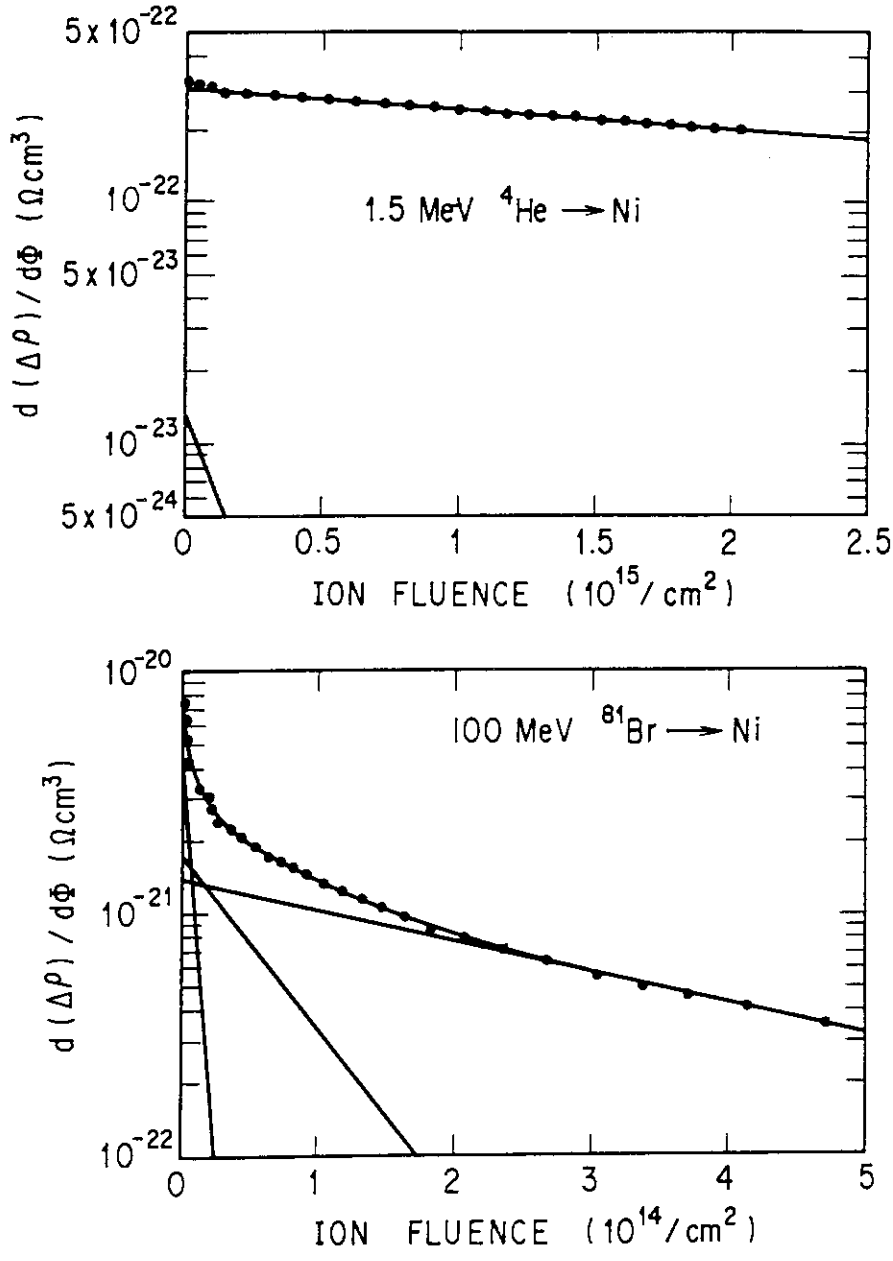

FIGURE 6 Defect production rates as functions of ion fluence for Ni irradiated with 1.5 MeV He ions and 100 MeV Br ions.

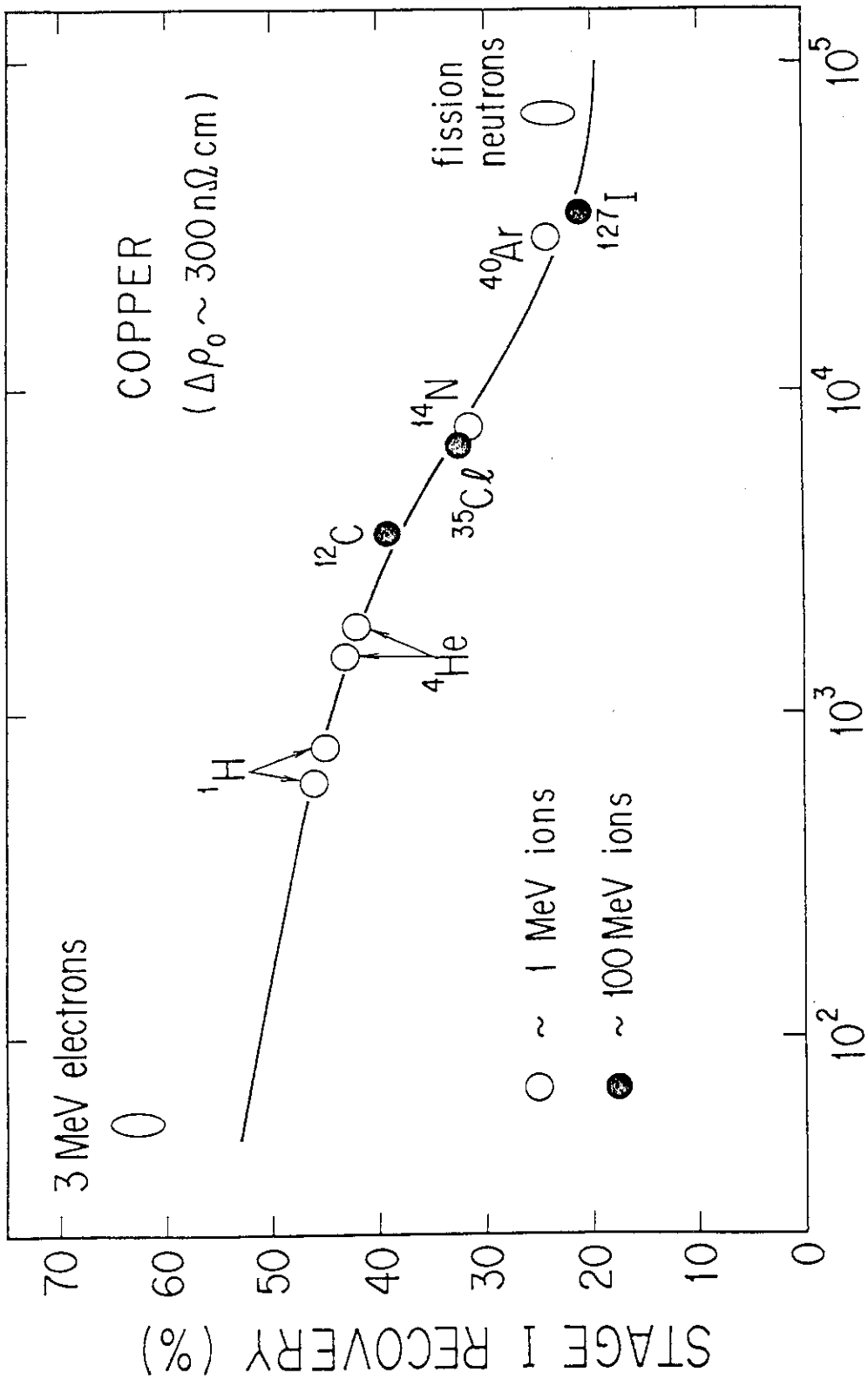

FIGURE 7 Fraction of stage I recovery in Cu as a function of the logarithm of PKA median energy after low temperature irradiations with electrons, various ions and neutrons. The defect concentration produced by irradiations is about 300 nΩ cm in resistivity unit.

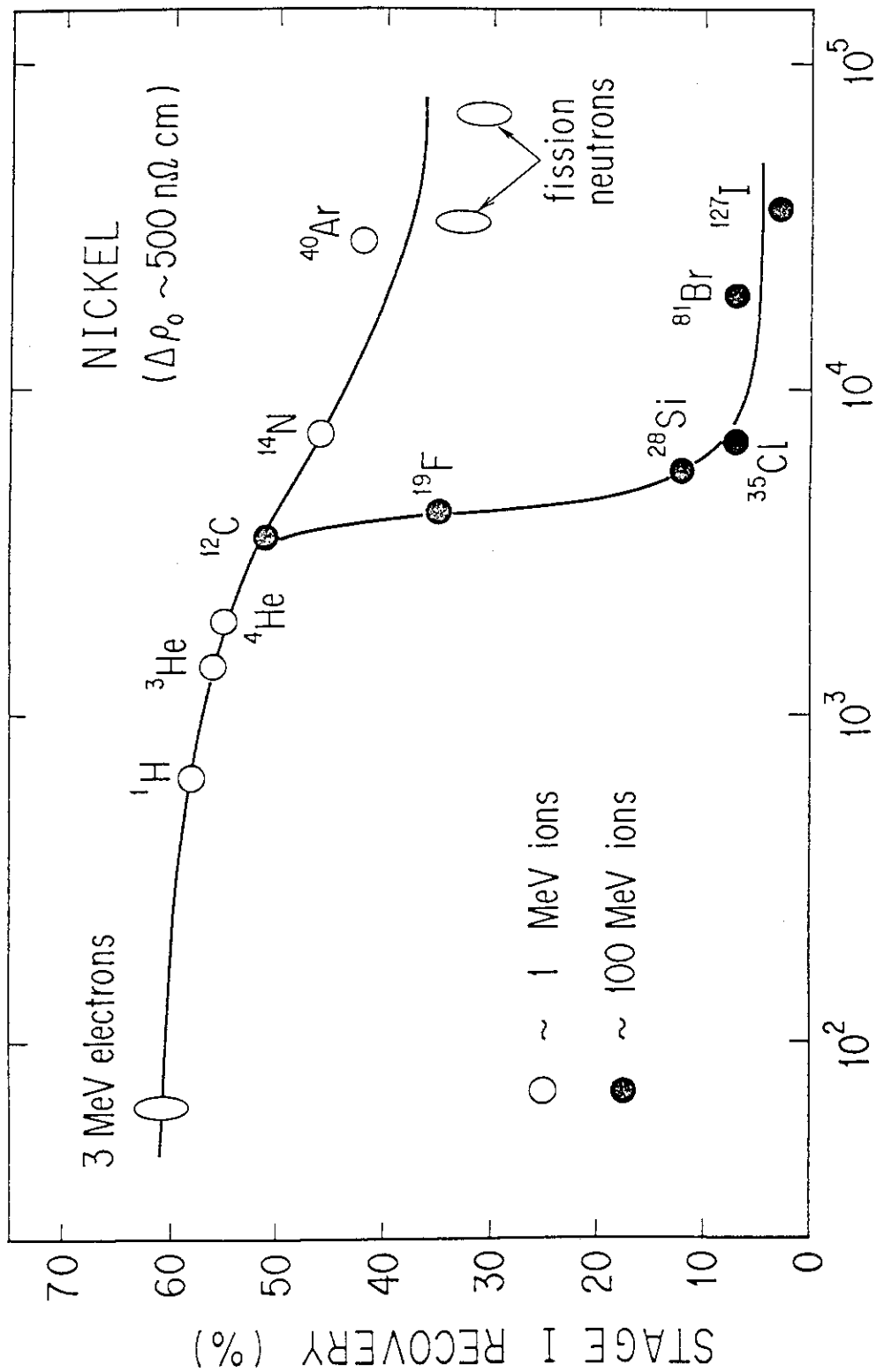

FIGURE 8 Fraction of stage I recovery in Ni as a function of the logarithm of PKA median energy after low temperature irradiations with electrons, various ions and neutrons. The defect concentration produced by irradiations is about 500 nΩ cm in resistivity unit.

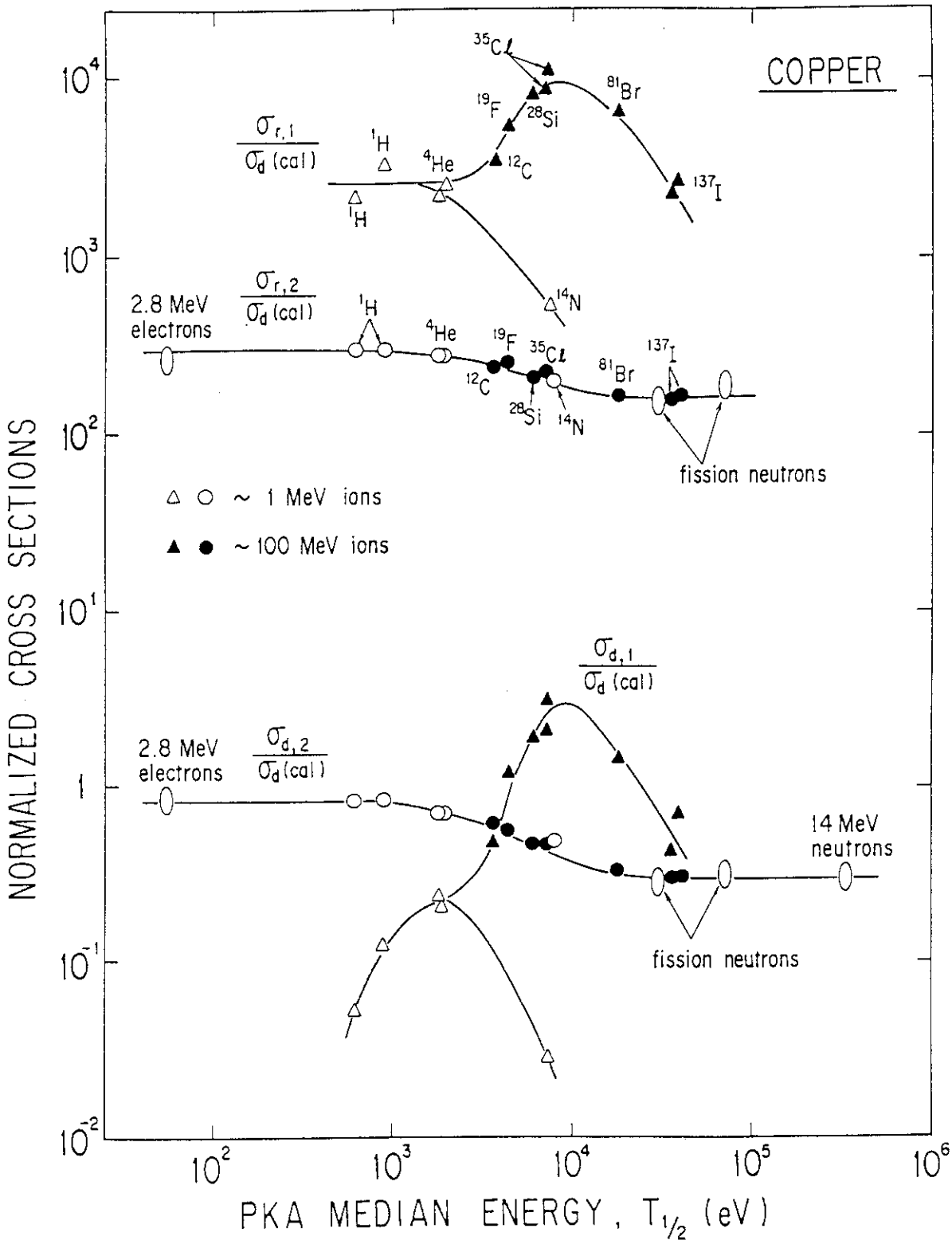

FIGURE 9 Normalized cross sections for defect production and radiation annealing of two types of defects in Cu as functions of the logarithm of PKA median energy for irradiations of electrons, various ions and neutrons.

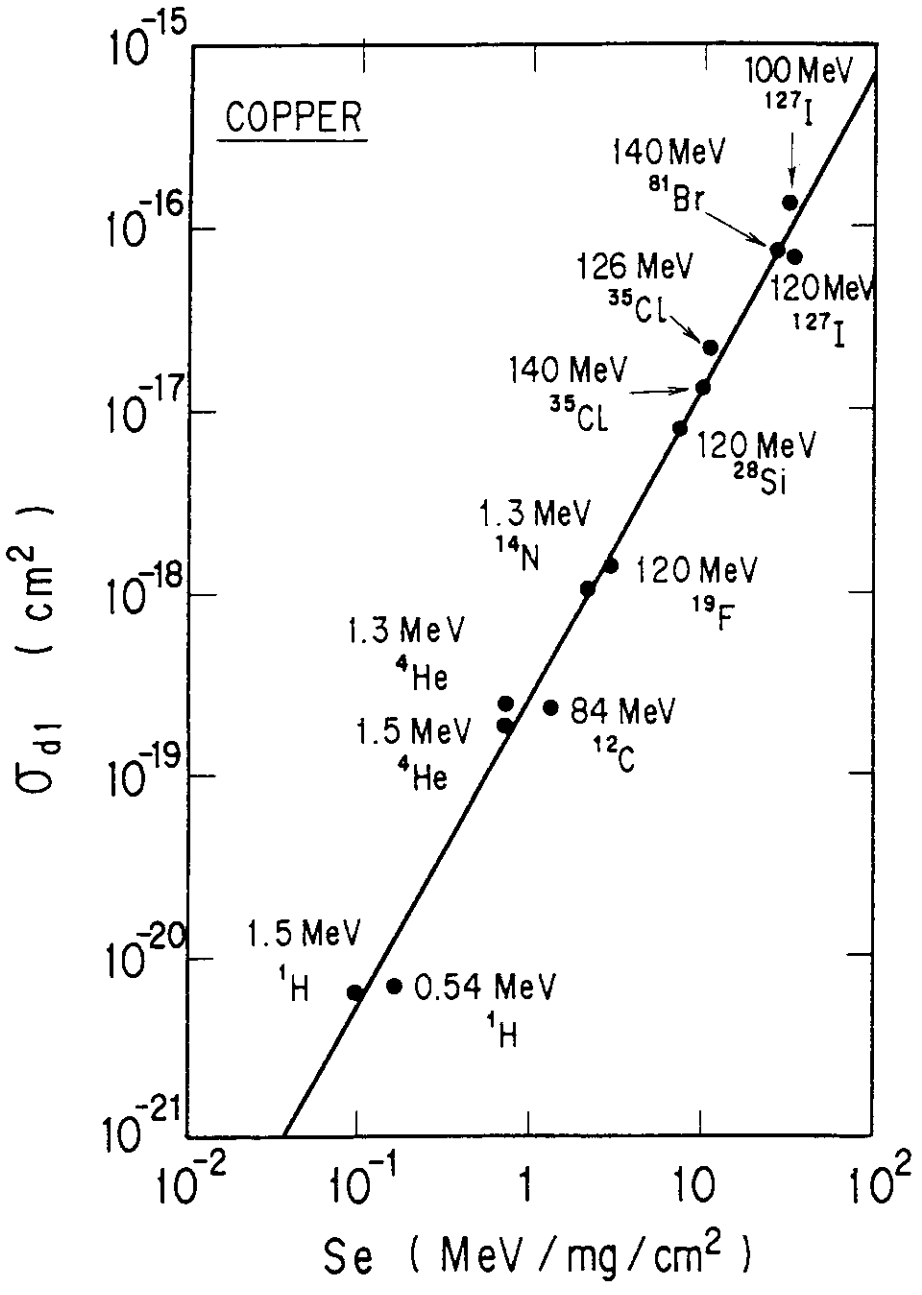

FIGURE 10 (a) Defect production cross sections of the defects of type 1 as a function of electronic stopping power for various ion irradiations to Cu.

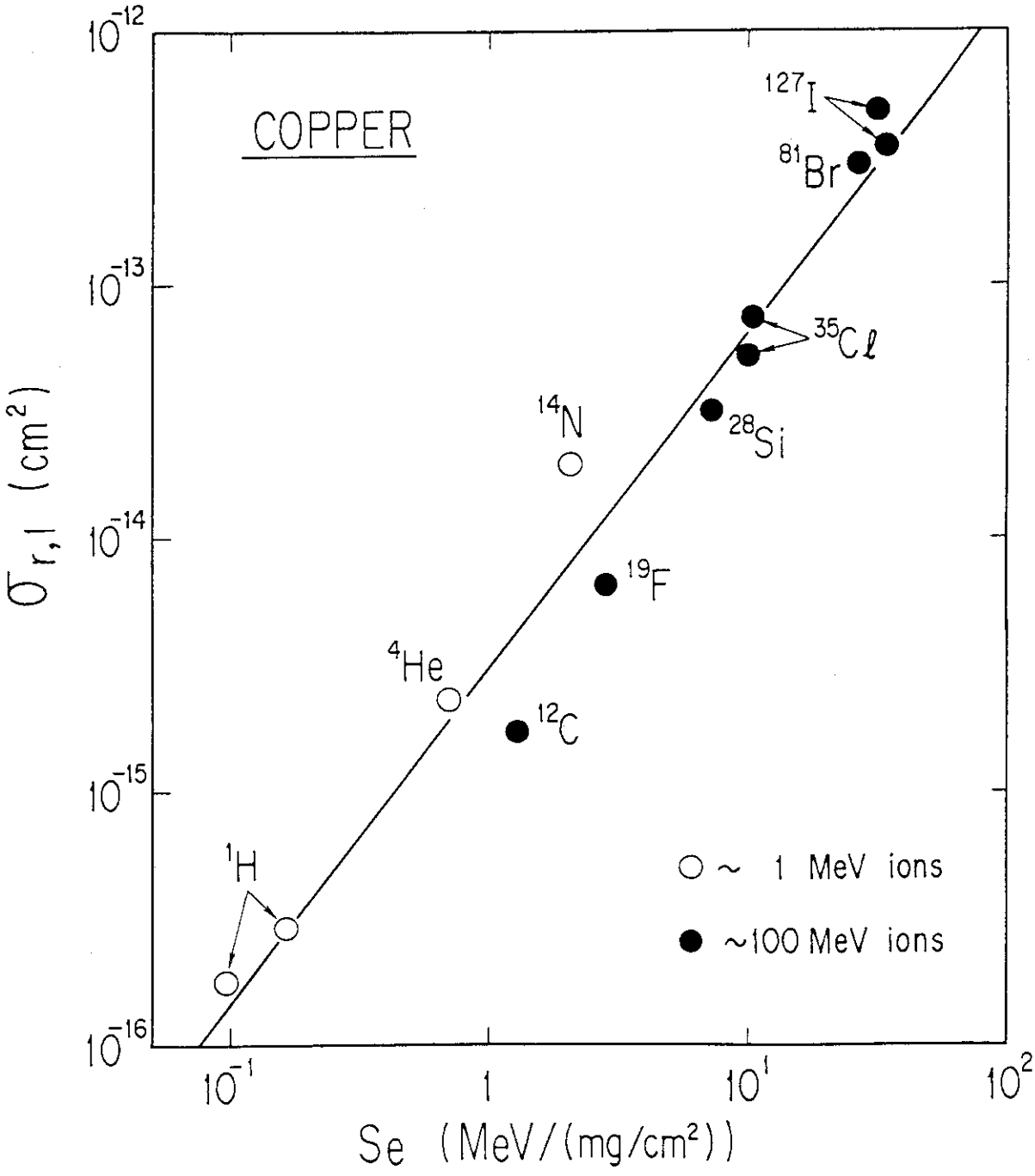

FIGURE 10 (b)Radiation annealing cross sections of the defects of type 1 as a function of electronic stopping power for various ion irradiations to Cu.

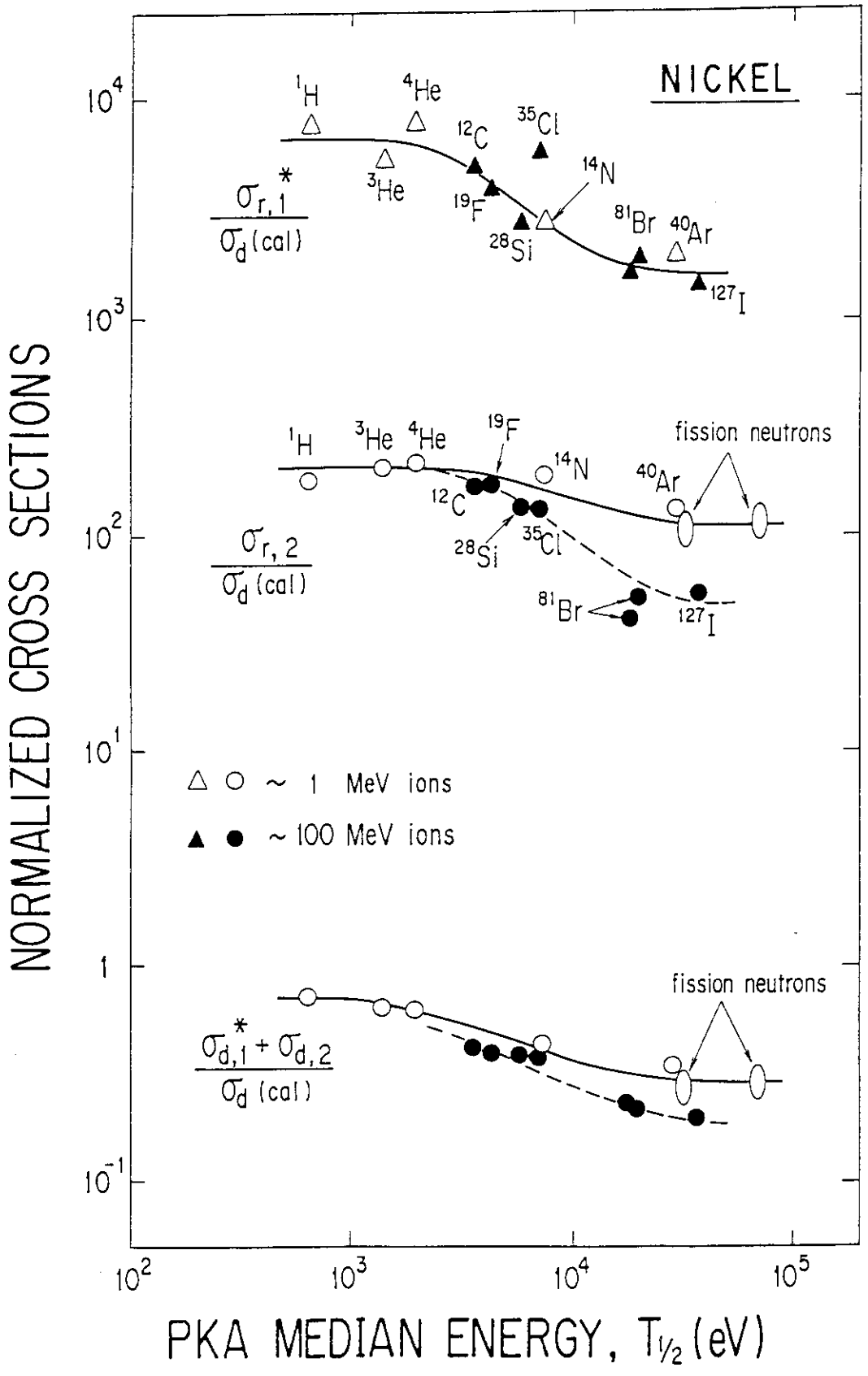

FIGURE 11 Normalized cross sections for defect production and radiation annealing of two types of defects in Ni as functions of the logarithm of PKA median energy for irradiations of various ions and neutrons.

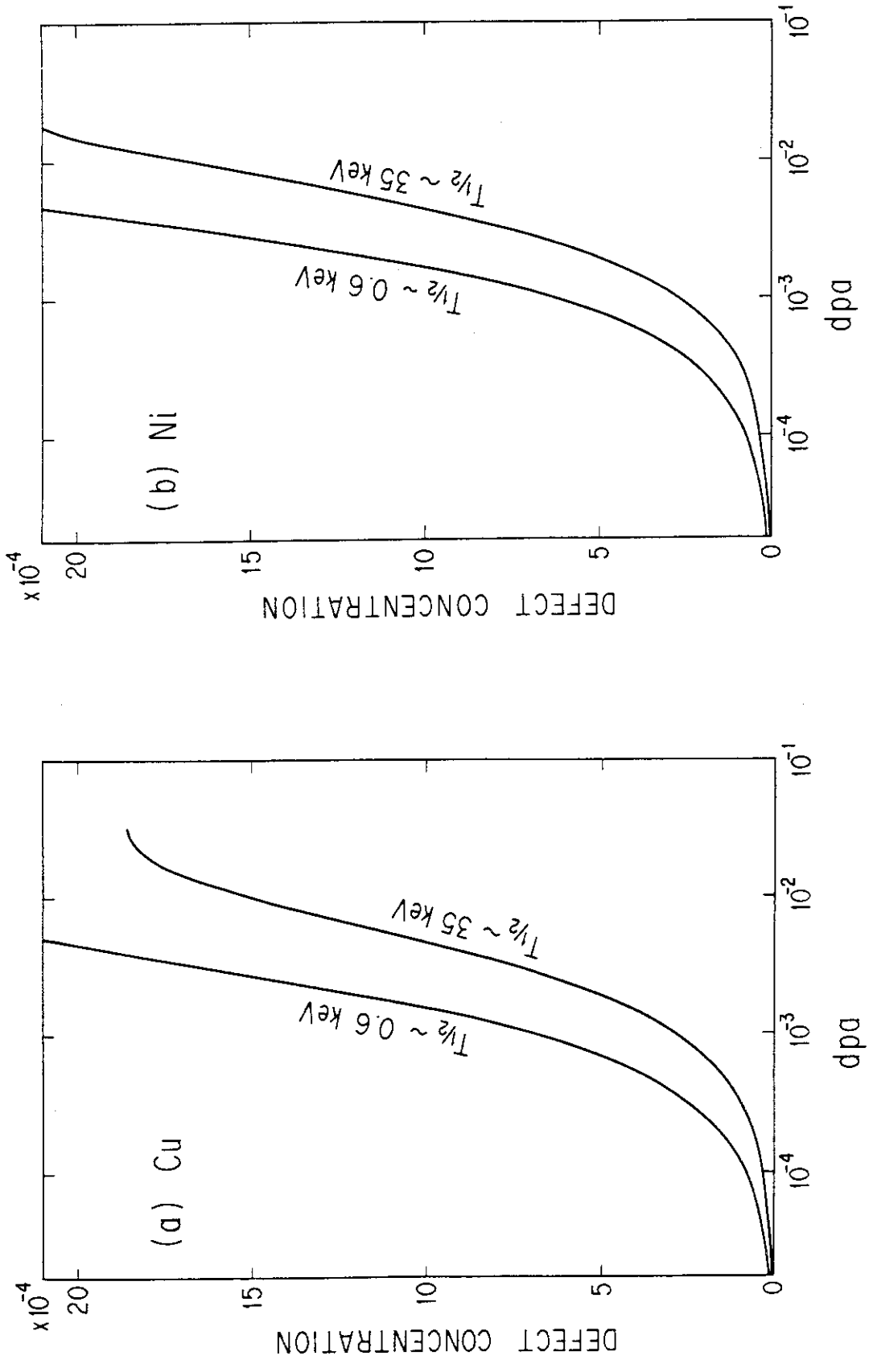

FIGURE 12 Damage accumulation (i. e. defect concentration) in (a) Cu and (b) Ni as a function of dpa with the PKA median energy as a parameter.